Department of Radio Science and Engineering

Multi-element Antennas for Mobile Communication Systems: Design, Evaluation and User Interactions

Azremi Abdullah Al-Hadi

A!

DOCTORAL DISSERTATIONS

Aalto University publication series
DOCTORAL DISSERTATIONS 146/2013

Multi-element Antennas for Mobile Communication Systems: Design, Evaluation and User Interactions

Azremi Abdullah Al-Hadi

A doctoral dissertation completed for the degree of Doctor of Science (Technology) to be defended, with the permission of the Aalto University School of Electrical Engineering, at a public examination held at the lecture hall S1 of the school on 8 November 2013 at 12 noon.

Aalto University
School of Electrical Engineering
Department of Radio Science and Engineering

Supervising professors
Prof. Pertti Vainikainen, until June 30, 2012
Assist. Prof. Ville Viikari, as of October 25, 2012

Thesis advisor
D.Sc (Tech.) Jari Holopainen

Preliminary examiners
Prof. Cyril Luxey, University of Nice Sophia-Antipolis, France
Dr. Tim Brown, University of Surrey, United Kingdom

Opponent
Prof. Gert F. Pedersen, Aalborg University, Denmark

Aalto University publication series
DOCTORAL DISSERTATIONS 146/2013

ISBN 978-952-60-5338-7
ISBN 978-952-60-5339-4 (pdf)
ISSN-L 1799-4934
ISSN 1799-4934 (printed)
ISSN 1799-4942 (pdf)
http://urn.fi/URN:ISBN:978-952-60-5339-4

Unigrafia Oy
Helsinki 2013

Finland

441 697
Printed matter

Aalto University

Abstract

Aalto University, P.O. Box 11000, FI-00076 Aalto www.aalto.fi

Author
Azremi Abdullah Al-Hadi

Name of the doctoral dissertation
Multi-element Antennas for Mobile Communication Systems: Design, Evaluation and User Interactions

Publisher School of Electrical Engineering

Unit Department of Radio Science and Engineering

Series Aalto University publication series DOCTORAL DISSERTATIONS 146/2013

Field of research Radio Engineering

Manuscript submitted 14 June 2013 **Date of the defence** 8 November 2013

Permission to publish granted (date) 11 September 2013 **Language** English

☐ **Monograph** ☒ **Article dissertation (summary + original articles)**

Abstract

Capacity improvement using Multiple-Input Multiple-Output (MIMO) technology necessitates multiple antennas at both transmitter and receiver ends. Antenna design challenges are related especially to mobile terminal, in which antennas need to be small, located relatively close to each other and interact with a user. Due to these limitations, mobile terminal antennas are potentially inefficient and do not provide a good MIMO performance. Traditional antenna design and characterization methods are not directly applicable to multiple antennas, and therefore research in these fields is needed.

This thesis contributes two topics. First, characterization methods of multiple antennas in compact mobile terminals are studied. In the studied methods, the effects of propagation environment and user on the multiple antenna performance are taken into account. The time-varying propagation environment and user's hand grip emulating the true scenario of the users in real-life environments are analyzed. In particular; different terminal orientations, hand grips and locations are investigated either with one or two hands holding the terminal.

Second, the thesis has scientific contribution on introducing novel multi-antenna structures with elements ranging from two to eight, and frequencies ranging from 900 MHz UHF to 3500 MHz LTE bands. Specifically, this thesis advances the design, evaluation and user interaction of multiple antennas in mobile terminals operating at the 3500 MHz. The proposed structures are shown to provide good diversity and MIMO performances. Selection of suitable antenna type and their locations on the terminal chassis are shown to be important. Based on author's experience, the proposed designs are particularly suitable for realizing a multi-element antenna structure that is tolerant to the user. Applicability of multiple antennas in compact mobile terminal for radio direction finding (RDF) is studied. Detailed analysis has also been carried out on the antenna topology on a mobile terminal and consideration of user interaction to ascertain the best use of antennas for such an application. It is found that ambiguity characterization method could be useful evaluation tool for designing a multi-antenna structure for RDF application.

Keywords multiple antennas, mobile antennas, diversity, MIMO systems, electromagnetic user interaction

ISBN (printed) 978-952-60-5338-7 **ISBN (pdf)** 978-952-60-5339-4

ISSN-L 1799-4934 **ISSN (printed)** 1799-4934 **ISSN (pdf)** 1799-4942

Location of publisher Helsinki **Location of printing** Helsinki **Year** 2013

Pages 167 **urn** http://urn.fi/URN:ISBN:978-952-60-5339-4

Preface

First and foremost, I would like to raise my infinite thanks to God, the Most Gracious and the Most Merciful. Alhamdulillah.

The research work presented in this thesis was performed between the years of November 2008 – May 2013 at Helsinki University of Technology (since 2010 Aalto University). The research works were carried out at the School of Electrical Engineering, Department of Radio Science and Engineering, under Radio Antenna and Propagation (RAP) group. The research and financial supports from Ministry of Higher Education Malaysia, Universiti Malaysia Perlis, SMARAD (Academy of Finland Centre of Excellence in Smart Radios and Wireless Research), and the Ella and Georg Ehrnrooth Foundation are gratefully acknowledged.

I would like to express my most sincere gratitude and appreciation to my supervisor, Professor Pertti Vainikainen for accepting me as one of his doctoral students. His trust, supports, encouragement and faithful guidance were the main reason for the emergence of this thesis. Assistant Professor Ville Viikari deserves warm thanks as well, for helping me through the fruitful discussions and guidance in the final phase of the dissertation processes.

I would like to thank the pre-examiners of my thesis, Professor Cyril Luxey and Dr. Tim Brown for their reviews and comments in order to improve the quality of the thesis. My appreciation also goes to Professor Gert Pedersen, who became an opponent during the public examination of my thesis.

Million of thanks to my instructor, Dr. Jari Holopainen, also to my other two seniors, Assistant Professor Katsuyuki Haneda and Dr. Clemens Icheln for the constructive discussions, scientific guidance and valuable help in my research work. In addition, I wish to acknowledge all of the other co-authors of my publications for their significant contributions to this the-

sis. For my colleagues and friends; Janne, Risto, Kimmo, Afroza, Dristy, Tero, Zhou, Mikko, Usman, Sathya, administrative staffs and everybody in the department; thank you very much. I am glad to know all of you. My Malaysian friends in Finland especially the Malaysian student's families, thank you for all the enjoyable moments that we shared together throughout the years.

Finally, I would like to express my warmest gratitude to my parents, Abdullah Al-Hadi Muhamed and Aishah Hassan, my parents-in-law, Mahmed Omar and Mek Yah Jusoh, and my siblings for their unconditional support, love and prayers. For my son Amir Hazeem Al-Hadi and daughter Anis Nur Iman, thank you for the love, patience, understanding and nicely behaved during papa's busy days. I love you both a lot! To Norsuria Mahmed, thank you for your love, prayers, patience, support, understanding and always by my side through my thick and thin. You are the exact person of this famous quote: 'Behind Every Successful Man There is a Woman!'.

Espoo, September 18, 2013,

Azremi Abdullah Al-Hadi

Contents

List of Publications

This thesis consists of an overview and of the following publications which are referred to in the text by their Roman numerals.

I A.A.H. Azremi, J. Ilvonen, C-H. Li, J. Holopainen and P. Vainikainen, "Influence of the user's hand on mutual coupling of dual-antenna structures on mobile terminal," In *Proceedings of the 6th European Conference on Antennas and Propagation*, 26-30 March, 2012, Prague, Czech Rep., pp. 1222-1226.

II A.A.H. Azremi, N. Jamaly, K. Haneda, C. Icheln and V. Viikari, "Design and measurement -based evaluation of multi-antenna mobile terminals for LTE 3500 MHz band," *Progress in Electromagnetic Research B*, vol. 53, pp. 241-266, 2013.

III A.A.H. Azremi, J. Ilvonen, R. Valkonen, J. Holopainen, O. Kivekäs, C. Icheln, and P. Vainikainen, "Coupling element –based dual-antenna structures with hand effects," *International Journal of Wireless Information Networks*, vol. 18, issue 3, pp. 146-157, 2011.

IV A.A.H. Azremi, V. Papamichael and P. Vainikainen, "Multi-antenna mobile terminal diversity performance in proximity to human hands under different propagation environment conditions," *Electronic Letters*, vol. 47, issue 22, pp. 1214-1215, 2011.

V A.A.H. Azremi, J. Toivanen, T. Laitinen, P. Vainikainen, X. Chen, N. Jamaly, J. Carlsson, P-S. Kildal and S. Pivnenko, "On diversity perfor-

mance of two-element coupling element based antenna structure for mobile terminal," In *Proceedings of the 4th European Conference on Antennas and Propagation*, 12-16 April, 2010, Barcelona, Spain, pp. 1-5.

VI A.A.H. Azremi, K. Haneda and P. Vainikainen, "Site-specific evaluation of a MIMO channel capacity for multi-antenna mobile terminals in proximity to a human hand," In *Proceedings of the 5th European Conference on Antennas and Propagation*, 11-15 April, 2011, Rome, Italy, pp. 538-542.

VII J. Ilvonen, O. Kivekäs, A.A.H. Azremi, R. Valkonen, J. Holopainen and P. Vainikainen, "Isolation improvement method for mobile terminal antennas at lower UHF band," In *Proceedings of the 5th European Conference on Antennas and Propagation*, 11-15 April, 2011, Rome, Italy, pp. 1307-1311.

VIII A.A.H. Azremi, M. Kyrö, J. Ilvonen, J. Holopainen, S. Ranvier, C. Icheln and P. Vainikainen, "Five-element inverted-F antenna array for MIMO communications and radio direction finding on mobile terminal," In *Loughborough Antenna and Propagation Conference*, 16-17 November, 2009, Loughborough, United Kingdom, pp. 557-560.

IX A.A.H. Azremi, M. Costa, V. Koivunen and P. Vainikainen, "Ambiguity analysis of isolation-based multi-antenna structures on mobile terminal," In *Proceedings of the 5th European Conference on Antennas and Propagation*, 11-15 April, 2011, Rome, Italy, pp. 552-556.

Author's Contribution

Publication I: "Influence of the user's hand on mutual coupling of dual-antenna structures on mobile terminal"

The idea was found by the author together with Dr. Jari Holopainen. The author had a leading role carrying out the simulations, analyzing the results and writing the paper. Mr. Janne Ilvonen and Dr. Chung-Huan Li participated in analyzing the results. Prof. Pertti Vainikainen supervised the work.

Publication II: "Design and measurement -based evaluation of multi-antenna mobile terminals for LTE 3500 MHz band"

The work was mainly done by the author. The author had the main responsibility for developing the idea and was responsible for writing the publication. Dr. Nima Jamaly participated in analyzing the results. Assist. Prof. Katsuyuki Haneda and Dr. Clemens Icheln instructed the work. Assist. Prof. Ville Viikari supervised the work.

Publication III: "Coupling element –based dual-antenna structures with hand effects"

The work was mainly done by the author. The author had the main responsibility for developing the idea. The author carried out the simulations and was responsible for writing the publication. Mr. Janne Ilvonen and Dr. Risto Valkonen helped with the simulations. Dr. Jari Holopainen, Dr. Outi Kivekäs and Dr. Clemens Icheln instructed the work. Prof. Pertti Vainikainen supervised the work.

Publication IV: "Multi-antenna mobile terminal diversity performance in proximity to human hands under different propagation environment conditions"

The author developed the main idea and had responsibility for writing the publication. Dr. Vasilis Papamichael participated in analyzing the results and in the writing of the manuscript. Prof. Pertti Vainikainen supervised the work.

Publication V: "On diversity performance of two-element coupling element based antenna structure for mobile terminal"

This is the result of collaborative work. The author carried out the simulations, performed measurements using different measurement techniques at different premises and was responsible for writing the publication. Dr. Juha Toivanen and Dr. Tommi Laitinen instructed the work. Prof. Pertti Vainikainen co-supervised the work.

Publication VI: "Site-specific evaluation of a MIMO channel capacity for multi-antenna mobile terminals in proximity to a human hand"

The author had the main idea and responsibility for writing the publication. Assist. Prof. Katsuyuki Haneda participated in analyzing the results and in the writing of the manuscript. Prof. Pertti Vainikainen supervised the work.

Publication VII: "Isolation improvement method for mobile terminal antennas at lower UHF band"

This is the result of collaborative work. The author participated in analyzing the results. Mr. Janne Ilvonen had the main responsibility for developing the idea and had the leading role of writing the manuscript. Dr. Outi Kivekäs instructed the work. Prof. Pertti Vainikainen supervised the work.

Publication VIII: "Five-element inverted-F antenna array for MIMO communications and radio direction finding on mobile terminal"

The idea was found by the author together with Prof. Pertti Vainikainen. The author carried out the simulations, performed the measurements and was responsible for writing the publication. Dr. Mikko Kyrö, Mr. Janne Ilvonen and Dr. Jari Holopainen helped in analyzing the results. Dr. Sylvain Ranvier and Dr. Clemens Icheln instructed the work. Prof. Pertti Vainikainen supervised the work.

Publication IX: "Ambiguity analysis of isolation-based multi-antenna structures on mobile terminal"

The author had the main idea and responsibility for writing the publication. Mr. Mario Costa participated in analyzing the results and in the writing of the paper. Prof. Visa Koivunen and Prof. Pertti Vainikainen supervised the work.

List of Abbreviations

1G	First generation
2G	Second generation
3G	Third generation
4G	Fourth generation
APS	Angular power spectrum
AUT	Antenna under test
BS	Base station
BuB	Balanced-unbalanced
CCE	Capacitive coupling element
CDF	Cumulative distribution function
CTIA	Cellular Telecommunications and Internet Association
DG	Diversity gain
DoA	Direction-of-arrival
EDGE	Enhanced data rates for global system for mobile communications evolution
FDTD	Finite-difference time-domain
GSC	Generalised selection combining
GPRS	General packet radio service
GPS	Global positioning system
GSM	Global system for mobile communications
IEEE	Institute of Electrical and Electronics Engineers
IFA	Inverted-F antenna
IP	Internet protocol
LOS	Line-of-sight
LTE	Long-term evolution
MA	Multi-element antennas
MEBAT	Measurement-based antenna test bed
MIMO	Multiple-input multiple-output

MRC	Maximal ratio combining
OTA	Over-the-air
PEC	Perfect electric conductor
PIFA	Planar inverted-F antenna
RC	Reverberation chamber
RDF	Radio direction finding
RF	Radio frequency
SAR	Specific absorption rate
SC	Selection combining
SISO	Single-input single-output
SNF	Spherical near-field
SNR	Signal-to-noise ratio
UHF	Ultra high frequencies (300 - 3000 MHz)
WLAN	Wireless local area network
WiMAX	Worldwide interoperability for microwave access

List of Symbols

ADG	apparent diversity gain
C	channel capacity
e^k_{emb}	embedded element efficiency of k-th element
e^k_{mp}	multiport matching efficiency of k-th element
e^k_{tot}	total embedded element efficiency of k-th element
$\mathbf{E}$	electric field vector
E	electrical field strength
E_θ	elevation electric field component
E_ϕ	azimuth electric field component
EDG	effective diversity gain
EM_{coup}	electromagnetic mutual coupling
$EM_{\text{coup,max}}$	maximum electromagnetic mutual coupling
G	gain of the antenna
G_{h}	horizontally polarized gain component
G_{v}	vertically polarized gain component
$\mathbf{H}$	magnetic field vector
H	magnetic field strength
m_{h}	mean elevation angle of horizontally polarized wave distribution
m_{v}	mean elevation angle of vertically polarized wave distribution
MEG	mean effective gain
MEG_0	mean effective gain of an ideal antenna
n_R	number of receiving antennas
n_T	number of transmitting antennas
P	power
P_{avs}	available power from a source
P_{imb}	power imbalance

P_{rad}	radiated power
P_{MRC}	cumulative distribution function using maximum ratio combining technique
P_{SC}	cumulative distribution function using selection combining technique
P_θ	elevation power component
P_ϕ	azimuth power component
$\mathbf{S}$	poynting vector
S_{jj}	input reflection coefficient (input from j-th element)
S_{jk}	transmission coefficient (from k-th to j-th element)
TSP	transferred signal power
XPD	cross-polarization discrimination
XPR	cross-polarization ratio

α	step in azimuth angle
β	step in elevation angle
γ	probability level
θ	elevation angle
θ_0	peak of elevation angle
λ	wavelength
ξ	eigenvalue of covariance matrix
ρ_{e}	envelope correlation
σ	angular spread
σ_{h}	angular spread of horizontally polarized wave distribution
σ_{v}	angular spread of vertically polarized wave distribution
ϕ	azimuth angle
Ω	solid angle

1. Introduction

1.1 Background

The evolution of cellular systems began in 1970s, starting with the first generation (1G) comprising of analog systems supporting basic voice transmission [1]. The second generation (2G) of cellular systems, global system for mobile communications (GSM) was developed in early 90's. The 2G systems provided digital encryption of the signal and improved the transmission quality and coverage. As the need for packet data arose, general packet radio service (GPRS) and enhanced data rates for GSM evolution (EDGE) technologies were introduced as an extension to the 2G systems. The advent of the 20^{th} century brought the third generation (3G) systems, which improved the data rates from several hundreds of kilobits per second (EDGE) to several megabits per second. This increased the internet usage from mobile devices, thereby fuelling the growth of the mobile broadband industry.

Recently introduced fourth generation (4G) systems provide even higher data rates enabling a wide range of telecommunication services, including mobile broadband internet access, internet protocol (IP) telephony, high-definition mobile TV, etc. The 4G system is aimed at providing peak data rates of up to 1 gigabit per second [2]. Two candidates of the 4G systems are commercially deployed around the world, namely long-term evolution (LTE) systems and worldwide interoperability for microwave access (WiMAX) technology [1, 3]. Both systems are based on packet-oriented communication. Meanwhile, new radio spectrum to accommodate new wireless systems is scarce and expensive. Therefore, available radio spectrum must be used efficiently without any increase on bandwidth or transmit power.

In a conventional communication link between the base station and a mobile terminal, a single antenna is used at both ends and thus is referred to as a single-input single-output (SISO) system. Capacity of a SISO system depends on the bandwidth, transmit power, and signal to noise ratio. The bandwidth and transmit power are limited by frequency regulations. In addition to noise, impairment due to the unavoidable phenomenon such as fading and shadowing exists in wireless communication systems. This limits the channel capacity of a SISO system.

In the late 1990s, multiple-input multiple-output (MIMO) systems that utilize multiple antennas at both ends of the link were introduced. This enables the use of multiple spatial channels at the same frequency. Hence, channel capacity of a MIMO system increases with the number of channels as compared to a SISO link. The number of spatial channels is limited to the number of antenna elements at an end of the link [4–7].

Implementation of MIMO in mobile communication system necessitates at least two antennas in one terminal. MIMO specific antenna design challenges are related to mutual coupling among antenna elements and degradation of antenna performance due to a user holding the mobile terminal [8–17]. The number of antennas to be incorporated in today's mobile terminal is restricted by the size of the terminal [18, 19]. This is contrary to a less severe space limitation at the base station. Moreover, the performance of a MIMO system depends not only on the antenna performance, but also on the propagation environment. The design of MIMO antennas for mobile terminals should also incorporate selection of optimal placement locations, topology, type and number of antenna elements. Therefore, a definitive and general conclusion on this subject has became major interest in antenna design community over the past few years [11, 12, 20–22].

1.2 Objective of the thesis

The main objective of this thesis is to provide novel and valuable insights for the design of multi-element antennas for mobile terminals. Particularly, the performance of the mobile terminal antennas in multipath environment is investigated in the presence of user's hand. The developed knowledge can be used to reduce mutual coupling between antenna elements and design robust antennas considering the effect of user's hand.

1.3 Contents and organization of the thesis

The main scientific results of this thesis are presented in articles [**I**] - [**IX**]. The thesis is divided into two parts. In the first part of the thesis, characterization methods of multi-element antennas in multipath propagation environment are studied in [**I**], [**II**], [**III**]. The performance of the multi-element antennas with different user's hand grips are analyzed extensively in [**I**], [**II**], [**III**], [**IV**], [**VI**]. The investigations are focused on understanding the effect of user's hand on multi-antenna performance metrics. The second part of the thesis is dedicated to the design of novel multi-antenna structures operating at the 900 MHz ultra high frequency (UHF) [**VII**] and 3500 MHz LTE and WiMAX technology bands [**II**], [**VIII**]. The design and performance investigation is extended to radio direction finding (RDF), which is a potential application of multi-element antennas [**VIII**], [**IX**]. In addition, measurement techniques to evaluate multi-antenna performance in multipath environment is investigated and compared in [**V**].

In this thesis, the main results are summarized into a larger scientific context. The summary is organized as follows. Chapter 2 summarizes the background and characterization methods of multi-element antennas. The effect of presence of user's hand on antenna characteristics, diversity and MIMO performances are studied in Chapter 3. Chapter 4 presents novel multi-antenna structures designed for diversity, MIMO and RDF in mobile terminals. This is followed by measurement techniques for multi-antenna structure in multipath environment. A summary of the publications describing the contributions of this thesis is presented in Chapter 5. Finally, Chapter 6 presents conclusions and possible ideas for future research.

1.4 Scientific contributions

The scientific merit of the thesis is in the design, analysis, performance evaluation and design rules for efficient multi-element antennas in a compact mobile terminal. The highlights are:

1. Systematic analysis and evaluation on the performance of multi-antenna configurations with different user's hand grips for diversity and MIMO applications [**I**], [**II**], [**III**], [**IV**], [**VI**].

2. An empirical investigation on the impact of integrating antenna elements from two to eight on MIMO terminal performances in the presence and absence of user's hand. The evaluation is performed using measurement -based propagation data [**II**].

3. Novel multi-antenna structure designs in compact bar- and clamshell-type mobile terminals are proposed. The realized structures are operational at the 900 MHz, 2000 MHz and 3500 MHz bands [**II**], [**III**], [**V**], [**VII**], [**VIII**].

4. Ambiguity characterization and analysis of multi-element antenna topology for RDF application in mobile terminals are performed [**VIII**], [**IX**].

5. Improving general understanding for designing multi-antenna structures in the presence and absence of user's hand [**II**], [**III**], [**IV**].

2. Multi-antenna characterization methods

Based on the antenna impedance matching, antennas can be divided into self-resonant and non-resonant structures. The antenna element of the mobile terminal is usually self-resonant, that is, the antenna is matched directly to the feed without additional matching circuitry [23, 24]. Non-resonant antennas have become more common over the past few years, as alternative solution in mobile terminal antennas [19, 25]. In these type of antennas, a reactive coupling element is made resonant with additional matching circuitry [26]. From the designer's point of view, non-resonant antennas are more flexible, because an electromagnetic problem is reduced into circuit analysis problem [27].

In general, the dimensions of mobile terminal antennas are electrically small, particularly in the lower UHF-band (below 1000 MHz). Typically, a significant portion of the power is radiated by the terminal chassis (ground plane of the printed circuit board) [28]. Hence, the terminal chassis dimensions at lower frequencies has an impact on the operation of the antenna [28–31].

Traditionally, the antenna in the mobile terminal is characterized by their size, impedance, bandwidth, efficiency and radiation pattern. Typically, the total efficiency is above 50%, reflection coefficient is smaller than -6 dB in the intended frequency band, and radiation is isotropic [23, 32]. These characteristics are partly useful when the performance of multi-element antennas are evaluated, since performance metrics that take the propagation environment into account is very important [5, 7, 33].

Diversity is used to mitigate multipath fading [4]. Particularly, multiple copies of the radio signal from different directions is used to enhance the link transmission reliability [7]. In contrast to this, spatial multiplexing uses distinct information streams over the propagation path to increase spectral efficiency [7, 34]. It is evident that the propagation environment

partly affects the ability and potential of a MIMO system [33, 35]. Therefore, antenna and propagation environment must be jointly considered when characterizing the performance of multi-element antennas in mobile terminals.

This chapter provides a basic overview of multi-antenna characteristics and performance of the antennas in multipath environment. Section 2.1 describes the characteristics of the multi-element antennas [**I**], [**II**], [**III**]. The performance metrics including the effect of the propagation environment are described in Section 2.2. Section 2.3 presents evaluation methodologies of the multi-element antennas in the propagation environment, either statistically [**III**], [**IV**] or based on measured propagation data [**II**], [**VI**].

2.1 Multi-element antenna characteristics

This section reviews multi-element antenna performance metrics that are extended from the traditional single-element antenna metrics. These parameters are useful in antenna design.

2.1.1 Mutual coupling

Since antenna elements are closely spaced in a compact mobile terminal, the resulting mutual coupling would not only cause unwanted interferences in multi-antenna systems, but also decrease their efficiency [36, 37]. In practice, the mutual coupling between antenna elements is expressed by scattering parameters, S_{jk} that denote voltage transfer from the k-th to j-th antenna ports. In [**I**], the concept of electromagnetic mutual coupling, EM_{coup} is used to generalize the maximum transducer gain of arbitrary two-port network for two-port antenna structure, when both elements are conjugate matched [38]. This can be used as a tool to evaluate the mutual coupling excluding the effect of impedance matching. The EM_{coup} is expressed by [**I**]:

$$EM_{\text{coup},jk}\,[\text{dB}] = 10 \cdot \log_{10}\left(\frac{|S_{jk}|}{|S_{kj}|}\left(A - \sqrt{A^2-1}\right)\right), \tag{2.1}$$

$$\Delta = S_{jj}S_{kk} - S_{jk}S_{kj}, \tag{2.2}$$

where,

$$A = \frac{1 - |S_{jj}|^2 - |S_{kk}|^2 + |\Delta|^2}{2\,|S_{jk}S_{kj}|}. \tag{2.3}$$

In (2.2) and (2.3), Δ and A are constants, and S_{jj}, S_{jk}, S_{kj} and S_{kk} are the scattering parameters for the *j*-th and *k*-th antenna elements. The maximum two-port transducer gain is the maximum power coupled between two ports of the network, which means in practice the worst-case free space coupling between antennas in a two-element antenna structure [**I**].

2.1.2 Efficiency

Antenna efficiency describes how efficiently an antenna can transform a guided wave into free-space radiation [39]. The efficiency is defined as the ratio between total radiated power P_{rad} and the accepted power P_{acc} at the terminal[1]. The total efficiency is defined as the ratio between the radiated power and the available power P_{avail}. This definition includes the losses due to impedance mismatch.

In a multiple antenna system with *N* antennas, when the *k*-th port is excited, part of the excitation signal is dissipated in the generators connected to the other ports provided that the antennas are not perfectly isolated. The total embedded element efficiency[2] of the *k*-th port, e_{tot}^k is defined as [36, 41, 42]:

$$e_{\text{tot}}^k = e_{\text{mp}}^k \cdot e_{\text{emb}}^k, \tag{2.4}$$

where e_{mp}^k is the multiport matching efficiency[3] and e_{emb}^k is the embedded element efficiency[4].

In general, the reduction of the antenna efficiency in multiple antenna system is attributed by the conductive and dielectric losses in the antenna, lossy objects in the vicinity of the antenna, and dissipation in the terminations of other antenna ports due to mutual coupling and reflection at its own excited port [36, 41, 43].

2.1.3 Polarization

In general, polarization of an antenna is given by the polarization pattern, that is the angular field distributions at θ- and ϕ- polarizations [23]. Cross polarization discrimination, *XPD* is defined as [18]:

$$XPD(\theta, \phi) = \frac{G_\theta(\theta, \phi)}{G_\phi(\theta, \phi)}, \tag{2.5}$$

[1] refer to IEEE Standard Definitions of Terms for Antennas [40].

[2] extension to a multiport version from the classical total efficiency used for single-element antenna.

[3] multiport version of the classical matching efficiency.

[4] multiport version of the classical radiation efficiency.

where $G_\theta(\theta,\phi)$ and $G_\phi(\theta,\phi)$ denote the gain patterns of the antenna obtained at the θ- and ϕ- polarization components, respectively. In a multiple antenna system with N antennas, the *XPD* is defined for each element.

2.2 Multi-element antenna in multipath environment

Let us consider a multi-element antenna in a multipath environment. The statistical power spectrum distributions of the incident field are described as:

$$P_\theta(\theta,\phi) = P_\theta(\theta)\, P_\theta(\phi), \tag{2.6}$$

$$P_\phi(\theta,\phi) = P_\phi(\theta)\, P_\phi(\phi). \tag{2.7}$$

$P_\theta(\theta,\phi)$ and $P_\phi(\theta,\phi)$ denote angular power spectrum (APS) of the incident wave at θ- and ϕ- polarizations, respectively. The ratio between the powers of two APSs defines the cross polarization ratio, *XPR* of the propagation environment [44]:

$$\boldsymbol{XPR} = \frac{P_\theta}{P_\phi}. \tag{2.8}$$

There are a variety of APS distributions and *XPR* values for different propagation scenarios [45]. The description of statistical distributions used in this thesis is described later in Section 2.3.

2.2.1 Mean effective gain

In a multipath environment, the ability of an antenna to receive electromagnetic power is quantified by mean effective gain, *MEG* [44]. It is defined as the ratio of the mean received power of a single antenna at the terminal to the mean received power of a single reference antenna. With dual-polarized isotropic antenna as the reference, *MEG* is given by [9,44]:

$$\boldsymbol{MEG} = \oint \left(\frac{\boldsymbol{XPR}}{1+\boldsymbol{XPR}} G_{\mathrm{v}}(\theta,\phi)\, P_\theta(\theta,\phi) + \frac{1}{1+\boldsymbol{XPR}} G_{\mathrm{h}}(\theta,\phi)\, P_\phi(\theta,\phi) \right) \sin\theta d\theta d\phi, \tag{2.9}$$

where $G_{\mathrm{v}}(\theta,\phi)$ and $G_{\mathrm{h}}(\theta,\phi)$ denote gain at vertical and horizontal polarizations at the terminal, respectively. In a multiple antenna system, each antenna element can be characterized by the *MEG*. The differences among the *MEG*s describe the power imbalance between antenna elements. For a good diversity performance, the power imbalance P_{imb} should meet the condition [4,46]:

$$P_{\mathrm{imb}} = \frac{|\boldsymbol{MEG}_j|}{|\boldsymbol{MEG}_k|} < 3 \text{ dB}. \tag{2.10}$$

2.2.2 Envelope correlation

Envelope correlation coefficient, $\rho_{\mathrm{e},jk}$ between the j-th and k-th element describes the correlation between the envelope of the signals at the two antenna ports. The correlation is affected by both APS and *XPR* of the propagation environment [4, 47]. It is a single value metric indicating the similarity in the voltages received by the two antennas, and is expressed by [10, 47, 48]:

$$\rho_{\mathrm{e},jk} = \frac{\left| \oint \left(\boldsymbol{XPR} \cdot E_{\theta j} \cdot E^*_{\theta k} \cdot P_\theta + E_{\phi j} \cdot E^*_{\phi k} \cdot P_\phi \right) \sin\theta d\theta d\phi \right|^2}{\prod\limits_{i=j,k} \oint \left(\boldsymbol{XPR} \cdot E_{\theta i} \cdot E^*_{\theta i} \cdot P_\theta + E_{\phi i} \cdot E^*_{\phi i} \cdot P_\phi \right) \sin\theta d\theta d\phi}, \tag{2.11}$$

where $E_\theta(\theta, \phi)$ and $E_\phi(\theta, \phi)$ denote the θ- and ϕ- components of the embedded element pattern[5] of an antenna element. The ρ_e ranges between 0 (no correlation) and 1 (full correlation). The envelope correlation below 0.3 ... 0.5 is typically regarded sufficient to facilitate uncorrelated signals [4, 49].

2.2.3 Diversity performance metrics

Good diversity performance necessitates that the envelope correlation is low and the received power is balanced equally between antenna elements [4, 18]. Diversity gain (DG) is defined as the improvement in a signal-to-noise ratio (SNR) achieved by combining the received signals of at least two antenna elements, compared to the SNR achieved by a reference antenna in the same environment.

The choice of the reference antenna results in different DG [13, 33]. Apparent diversity gain, *ADG* is used when the comparison is made to the best element of the diversity antenna, that is the antenna element with the strongest average received signal in the same environment [13, 36, 50]. The result is expressed as the probability that the instantaneous resultant SNR, γ is below a predefined level x, $P(\gamma \leq x)$. An effective diversity gain, *EDG* is a more realistic measure than the *ADG*, which is described by [13, 50]:

$$\boldsymbol{EDG} = \boldsymbol{ADG} \,.\, \max_k \left\{ e_{\mathrm{tot},k} \right\}. \tag{2.12}$$

Fig. 2.1 shows a cumulative distribution function (CDF) of the received signals as a function of SNR. The definition of *ADG* and *EDG* is also shown in Fig. 2.1. *EDG* represents the diversity gain relative to a single lossless reference antenna. It takes into account reduction in embedded

[5] multiport version of the classical radiation pattern, when the foregoing port is excited [36].

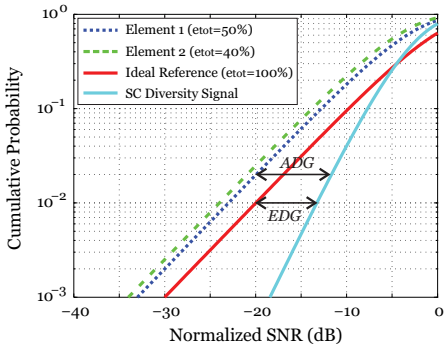

Figure 2.1. Definitions of *ADG* and *EDG* for an arbitrary two-element antenna in uniform environment. The two elements are uncorrelated, $\rho_{e,12} = 0$.

element efficiency due to the mutual coupling between elements of the diversity antenna [50].

The received signals at individual antenna element can be combined in several ways resulting in different levels of complexity. Well-known techniques are selection combining, switched combining, equal gain combining and maximum ratio combining [18, 51]. In this thesis, we consider selection combining (SC) and maximum ratio combining (MRC). With regard to their performance, SC is inferior to MRC, at the expense of an increased system complexity. In this thesis, SNR is generalized to *MEG* (2.9), by assuming that the noise level is the same across all antenna elements [33].

For a two-element antenna system, a CDF of the combined signal using SC technique, $P_{\mathrm{SC},2}$ is given by [52]:

$$P_{\mathrm{SC},2}\left(\gamma \leq x\right) = 1 - \exp\left(-\tfrac{x}{\mathit{MEG}_1}\right) Q\left(a, \sqrt{\rho_{e,12}}\, b\right) - \exp\left(\tfrac{x}{\mathit{MEG}_2}\right) Q\left(\sqrt{\rho_{e,12}}\, a, b\right), \tag{2.13}$$

where

$$a = \sqrt{\frac{2x}{\mathit{MEG}_2\left(1 + \rho_{e,12}\right)}}, \quad b = \sqrt{\frac{2x}{\mathit{MEG}_1\left(1 - \rho_{e,12}\right)}}. \tag{2.14}$$

$\rho_{e,12}$ is the envelope correlation (2.11) between the first and the second element. $Q(\cdot)$ refers to the Marcum Q-function. When using MRC, the CDF of the combined signal, $P_{\mathrm{MRC},2}$ is given by [52]:

$$P_{\mathrm{MRC},2}\left(\gamma \leq x\right) = \frac{1}{\xi_1 - \xi_2} \times \left[\xi_1 \left\{1 - \exp\left(-\frac{x}{\xi_1}\right)\right\} - \xi_2 \left\{1 - \exp\left(-\frac{x}{\xi_2}\right)\right\}\right], \tag{2.15}$$

where ξ refers to the associated eigenvalue of signals covariance matrix

R, which is formulated by:

$$\mathbf{R} = \mathit{MEG}_0 \begin{bmatrix} \mathit{MEG}_1 & (\mathit{MEG}_1\, \mathit{MEG}_2\, \rho_{\mathrm{e},12})^{1/2} \\ (\mathit{MEG}_1\, \mathit{MEG}_2\, \rho_{\mathrm{e},12})^{1/2} & \mathit{MEG}_2 \end{bmatrix}, \quad (2.16)$$

where MEG_0 refers to the *MEG* of a dual-polarized isotropic antenna with unity radiation efficiency, which is used as a reference for calculating diversity gain.

The CDF of the MRC output for an arbitrary N-element antenna is calculated by [52, 53]:

$$P_{\mathrm{MRC},N}\left(\gamma \leq x\right) = 1 - \sum_{j=1}^{N} \frac{\lambda_k^{N-1} \exp\left(-x/\lambda_j\right)}{\prod_{k\neq j}^{N}\left(\lambda_j - \lambda_k\right)}, \quad (2.17)$$

where λ_j $(j = 1, 2...N)$ is the j-th eigenvalue of the $N \times N$ signals covariance matrix Λ. The element of the matrix Λ is given as:

$$\Lambda_{jk} = \mathit{MEG}_0\, \rho_{\mathrm{e},jk} \sqrt{\mathit{MEG}_j\, \mathit{MEG}_k}. \quad (2.18)$$

2.2.4 MIMO performance metrics

Shannon channel capacity equation can be used to obtain the ultimate capacity of the MIMO link performance [54]. In this thesis, the MIMO channel capacity on the conditions where the channel is unknown at the base station, but known at the terminal is used. The instantaneous MIMO channel capacity for the i-th terminal location, $C^{(i)}$ is defined as [55–57]:

$$C^{(i)} = \log_2 \left[\det \left(\mathbf{I} + \frac{\rho}{n_T} \frac{\mathbf{H}_{\mathrm{AUT}}^{(i)} (\mathbf{H}_{\mathrm{AUT}}^{(i)})^{\mathrm{H}}}{P_{\mathrm{norm}}} \right) \right], \quad (2.19)$$

where $\mathbf{I}$ is an identity matrix, ρ is the mean signal-to-noise ratio (SNR) at the mobile terminal, n_T is the number of transmitting antennas and $(.)^{\mathrm{H}}$ denotes the Hermitian transpose. MIMO channel matrix, $\mathbf{H}_{\mathrm{AUT}}$, includes the effect of embedded element patterns at both base and mobile stations. The channel matrix $\mathbf{H}$, whose size is $n_R \times n_T$ (n_R is the number of receiving antennas), represent a scattering matrix between different transmit and received antennas. A reference antenna gives the power for normalization, P_{norm}, which is calculated at each mobile terminal location and expressed by [55]:

$$P_{\mathrm{norm}} = \frac{1}{n_T n_R} \left\| \mathbf{H}_{\mathrm{ref}}^{(i)} \right\|_F^2, \quad (2.20)$$

where $\|.\|_F$ is the Frobenius norm. $\mathbf{H}_{\mathrm{ref}}$ is the channel matrix with reference antennas at the base station and mobile terminal, respectively. In

[**II**] and [**VI**], an isotropic antenna is used to give the reference power for normalization in the evaluation of MIMO channel capacity.

The MIMO channel capacity is also affected by the distribution of the eigenvalues of $\mathbf{H}_{\mathrm{AUT}}^{(i)}(\mathbf{H}_{\mathrm{AUT}}^{(i)})^{\mathrm{H}}$ [5]. Theoretically, an increase of relative spread between the eigenvalues indicates an increase in spatial correlation between antenna elements [58].

The ability to transfer signal power between the two ends of the link depends on the losses in a propagation environment, antenna radiation properties and orientation. The instantaneous transferred signal power, *TSP* of the multi-antenna system is defined as [56]:

$$TSP_{\mathrm{AUT}}^{(i)} = \frac{\left\|\mathbf{H}_{\mathrm{AUT}}^{(i)}\right\|_F^2}{\left\|\mathbf{H}_{\mathrm{ref}}^{(i)}\right\|_F^2}. \tag{2.21}$$

2.3 Methods for performance evaluation in uniform and non-uniform multipath environments

Isotropic uniform environment has been widely used as an extreme reference environment, where the performance considerably depends on the total efficiencies of the studied multi-antenna structures [59]. In this environment, the incident power is equally split between the two orthogonal polarizations (balanced polarization) and the angular power distribution is constant ($P_\theta(\Omega) = P_\phi(\Omega) = \frac{1}{4\pi}$ and *XPR* = 0 dB). Indoor environments with strong scattering can be approximated as the uniform environment [4, 18].

A real-life environment is in between an ideal free space, i.e., pure line-of-sight (LOS), and the isotropic uniform environment in terms of amount of scattering [59]. When the real-life propagation environment is modelled, the incident signal is often taken from a well-known distribution, such as Gaussian, Laplacian, general Double-Exponential and Rectangular distributions [9, 10, 18, 45, 57, 60, 61]. Performing series of propagation measurements for characterization and evaluation of different multi-antenna designs is very expensive, and laborious [15, 17, 62, 63].

The measurement-based evaluation reviewed in this thesis is based on the principle of combining simulated embedded patterns with multiple plane waves representing measured propagation environment. A tool called measurement-based antenna test bed (MEBAT) for this purpose was developed and discussed in detailed in [55, 64], and was used exten-

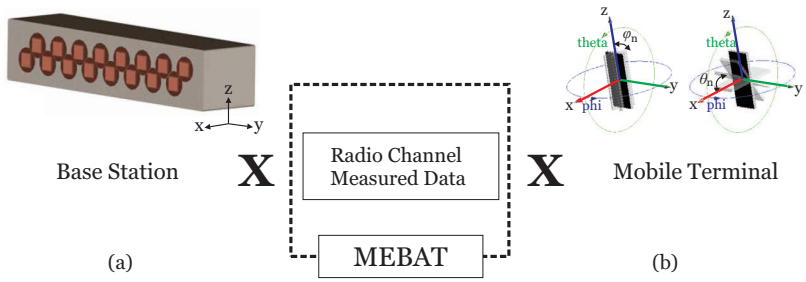

Figure 2.2. Block diagram of MEBAT consisting of embedded patterns of studied multi-antenna structures at (a) base station, and (b) mobile station. **X** denotes multiplication.

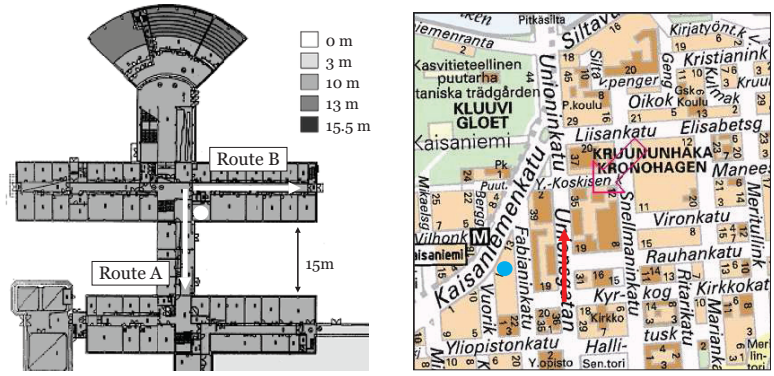

Figure 2.3. (a) Indoor propagation routes include obstructed LOS (Route A) and non LOS (Route B) scenarios, and (b) outdoor microcellular route in Helsinki city centre. The circle represents base station location while the arrows are mobile routes [**II**, **VI**].

sively for the performance prediction in [57].

Basic working principle of the MEBAT is illustrated in Fig. 2.2. The angular power spectrum (APS) of an environment under interest is measured with a channel sounder [45, 65]. The measured propagation environment is composed of a set of discrete plane waves, that are independent of antenna arrays used in the measurements. A MIMO channel matrix $\mathbf{H}_{\mathrm{AUT}}$ (2.19) is obtained by combining the embedded patterns of multi-antenna structure at the base station and the mobile terminal with measured plane waves.

In [**II**] and [**VI**], arbitrary rotation effects (see Fig. 2.2(b)) is simulated at each mobile location by rotating the radiation pattern in $\phi = 60^\circ$ steps in azimuth plane, at each elevation angle $\theta = 30^\circ$ and $\theta = 60^\circ$, respectively. Then, the MIMO channel matrix is computed at each mobile terminal location along the propagation route, that is shown in Fig. 2.3. In this the-

sis, experimental propagation data obtained at the 2154 and 5300 MHz frequencies are used for performance analysis and evaluation of multi-antenna mobile terminals.

3. Performance in presence of a user

The number of investigations on multi-element mobile terminal antenna performance due to the presence of user's hand have been increasing over the past few years [8–10, 13, 17, 61, 66–74]. The user's hand causes impedance mismatch, change of radiation pattern and reduction in total efficiency of the antenna [75–79]. This is mainly due to dielectric losses in the user's hand. In addition, specific hand grip has a major effect on the antenna performance [80, 81]. Since the mobile terminal is a consumer product, the maximum radiation exposure to the end user of the terminal is limited by regulations. Therefore, the exposure is evaluated with a standardized test plan defined by CTIA[1] [82].

The presence of user's hand alters the antenna impedance depending upon operational frequencies and wavemodes of the terminal chassis [83, 84]. At high frequencies (above 3000 MHz), the radiation from the antenna itself is dominant compared to the terminal chassis resonances [26]. For this reason, antenna dimension and geometry are important in the evaluation.

Different antenna-types from both self-resonant and non-resonant structures covering different frequencies are investigated in this thesis. Therefore, internal state-of-the-art mobile antennas such as self-resonant planar inverted-F antennas (PIFAs), inverted-F antennas (IFAs), and non-resonant capacitive coupling element (CCE) antennas are designed and used in the evaluation.

Fig. 3.1 illustrates various types of hand grips used in the evaluation, that is, one hand grip in talk or data mode [**II**], [**III**], [**IV**], [**VI**] and two hand grips for browsing mode [**II**], [**IV**]. Five different vertical offset positions of talk-grip along terminal chassis are investigated across studied

[1] CTIA-The Wireless Association® is an international non-profit membership organization that has represented the wireless communications industry since 1984.

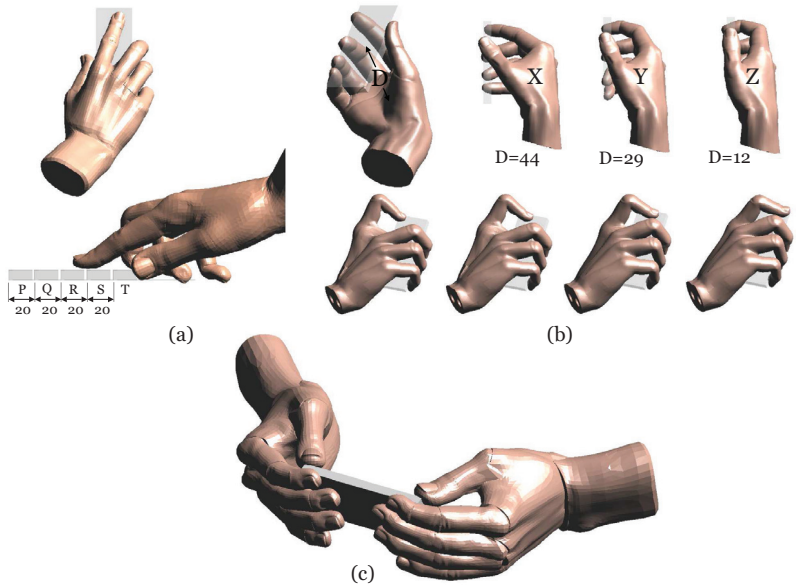

Figure 3.1. Hand phantom models for one hand grip in (a) talk mode, (b) data mode, and for two hands grip in (c) browsing mode. D is the distance between palm and the terminal chassis. Effects of different index finger positions, and palm-terminal distances are shown next to each one hand phantom models, respectively. All units are in millimeter.

multi-antenna structures, where locations are shown in Fig. 3.1(a). In this grip, the distance between the center of the palm to the terminal chassis is 42 mm. The effect of palm-phone distance, D defined in Fig. 3.1(b) is also investigated. In this thesis, the presence of other parts of the human body is neglected throughout the investigations because the hand is typically very close to the antenna and therefore dominates.

This chapter discusses the performance of multi-antenna structures in the presence of user's hand considering the metrics defined in Chapter 2. Section 3.1 investigates the effects of user's hand on near-field distributions of a multi-antenna structure in mobile terminal [**I**]. The impact of user's hand on the diversity and MIMO performances are presented in Sections 3.2 and 3.3, respectively [**II**], [**III**], [**IV**], [**VI**]. In Section 3.4, impact of incorporating antennas in mobile terminal on MIMO performance are investigated [**II**]. Finally, locations for antennas that tolerant to the effect of the user's hand is proposed in Section 3.5.

3.1 User effect on multi-antenna characteristics and near-field distributions

Study on near-field distributions of multi-element antennas in the presence of user's hand was the main interest of the work in [**I**]. The PIFA is selected to investigate multi-antenna performance at wide range of operating frequencies, that is with two-element antenna structures operating at 900, 2000, 3500 and 5300 MHz. Location of the index finger and its touching area on the mobile terminal were found to affect antenna performance significantly [81, 85]. Hand grip in the data mode shown in Fig. 3.1(b) is used to model these two main hand effects.

It is found that the average reduction of total embedded efficiencies (2.4) due to the user's hand are -6.5, -2.5, -2.1 and -1.8 dB for 900, 2000, 3500 and 5300 MHz PIFA structures, respectively. The calculated EM_{coup} (2.1) in the presence of user's hand indicates the worst-case mutual coupling that is reached when both antenna elements are simultaneously conjugate-matched. The maximum difference between EM_{coup} in the presence and absence of user' hand defines the maximum electromagnetic mutual coupling, $\triangle EM_{\text{coup,max}}$. In [**I**], the difference is computed within 200 MHz bandwidth. The $\triangle EM_{\text{coup,max}}$ is presented as a function of index finger locations shown in Fig. 3.2.

In the reactive near-field region of the two-element antenna structures shown in Fig. 3.2, there exists low $\triangle EM_{\text{coup}}$ with an average of -8 dB at 900 MHz, contrary to high $\triangle EM_{\text{coup}}$ with an average of 2 dB for structures

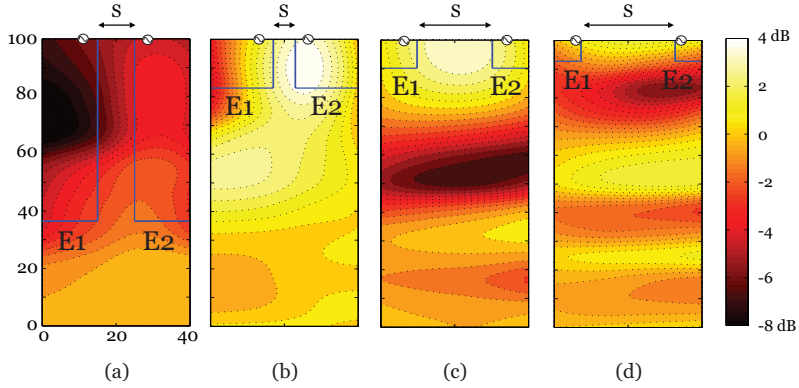

Figure 3.2. $\triangle EM_{\text{coup,max}}$ of the two-element PIFA as a function of the index finger locations at (a) 900 MHz (S = 0.03λ), (b) 2000 MHz (S = 0.04λ), (c) 3500 MHz (S = 0.24λ) and (d) 5300 MHz (S = 0.45λ). The solid blue lines represent edges (top view) of the two-element PIFA. 'S' denotes edge-to-edge separation between the two elements. E1 and E2 denote element 1 and element 2, respectively. See [**I**] for the details of the antenna dimension.

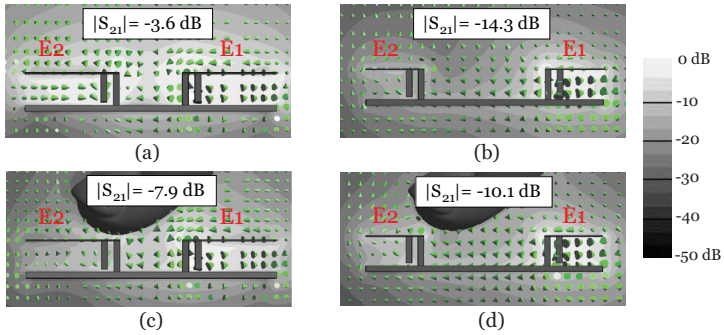

Figure 3.3. Plane-cut of S(r), when E1 is excited and E2 is terminated with 50 ohm, in the absence of hand at (a) 900 MHz, (b) 3500 MHz, and in the presence of user's hand at (c) 900 MHz and (d) 3500 MHz. The corresponding values of mutual coupling are shown in the box [**I**].

above 2000 MHz. The negative $\triangle EM_{\text{coup}}$ means that the mutual coupling is decreased when hand is present. From the circuit point of view, this indicates that the power is reflected from the feed port of the antennas whereas from the electromagnetic field point of view, it is related to power flow. The power flow is defined by the complex Poynting vector, **S** given as [38]:

$$\mathbf{S}(\mathbf{r}) = \frac{1}{2}\mathrm{Re}\left(\mathbf{E}(\mathbf{r}) \times \mathbf{H}^{*}(\mathbf{r})\right), \tag{3.1}$$

Fig. 3.3 illustrates the effects of index finger on Poynting field distribution of the dual-PIFA structures at 900 and 3500 MHz, respectively. In Fig. 3.3(a), it is shown that at 900 MHz, there exists high mutual coupling between the two antenna elements due to small inter-element spacing and coupling through the terminal chassis, as expected. In Fig. 3.3(c), larger power is absorbed by the index finger, while less power is coupled to E2. At higher frequencies, the power is scattered and reflected back to E2 (when E1 is excited), as shown in Figs. 3.3(b) and 3.3(d), respectively. In addition, different near-field distributions are due to the fact that the antenna-chassis coupling behaves differently at different frequencies [28, 29, 31, 86].

It is shown that the two-element structures exhibit up to 10 dB variations in the mutual coupling, depending on the hand and index finger locations. The Poynting vector is used for the first time as a tool to understand the behavior of the mutual coupling in the two-element structures, in the presence of user's hand.

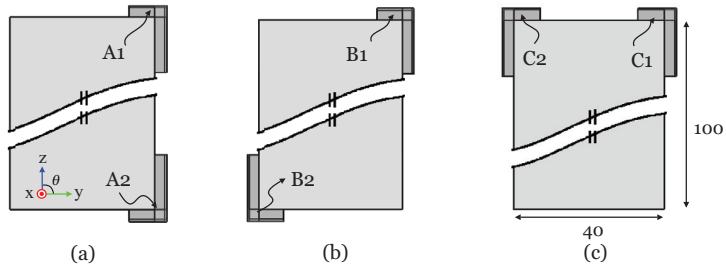

Figure 3.4. Two-element antenna configurations; (a) configuration A (vertically oriented), (b) configuration B (diagonally oriented) and (c) configuration C (adjacently oriented) antennas. See [**III**] for the details of the antenna dimension.

3.2 User effect on envelope correlation, power imbalance and diversity performances

In [**III**], two-element antenna configurations are designed at 2000 MHz with similar CCE elements but placed at different chassis corners. The corners are selected because they are an optimal location to couple with the dominating characteristic wavemodes of the terminal chassis [25, 87]. The configurations are illustrated in Fig. 3.4. The impact of the hand on envelope correlation, power imbalance and diversity performance of these configurations are investigated.

As described in Section 2.2.1, the power imbalance by means of difference between *MEG*s of the two branches is investigated. For simplicity, the propagation environment is modelled as isotropic uniform one. In the presence of user's hand, the imbalance between the two branches can occur when one of antenna elements is obstructed and covered by some parts of the user's hand. The degree of *MEG* imbalance, P_{imb} can be expressed by [**III**]:

$$P_{\text{imb}}\,[\text{dB}] = \mathit{MEG}_{\text{WithHand},i}\,[\text{dBi}] - \mathit{MEG}_{\text{WithHand},j}\,[\text{dBi}]\,, \tag{3.2}$$

where $\mathit{MEG}_{\text{WithHand},i}$ corresponds to the best branch power of the two-element antenna structure, and $\mathit{MEG}_{\text{WithHand},j}$ is the power of the other branch, when both antenna elements are in the presence of user's hand.

Fig. 3.5(a) shows that the envelope correlations are very small for all tested hand phantom positions, and meet the criterion of $\rho_{\text{e}} < 0.5$ [4, 88]. Due to a fairly large separation between the two elements in configuration A and B, a very low envelope correlation is achieved. Meanwhile, configuration C has higher average of envelope correlation compared to others, but still ρ_{e} is below 0.5. This is due to close separation between

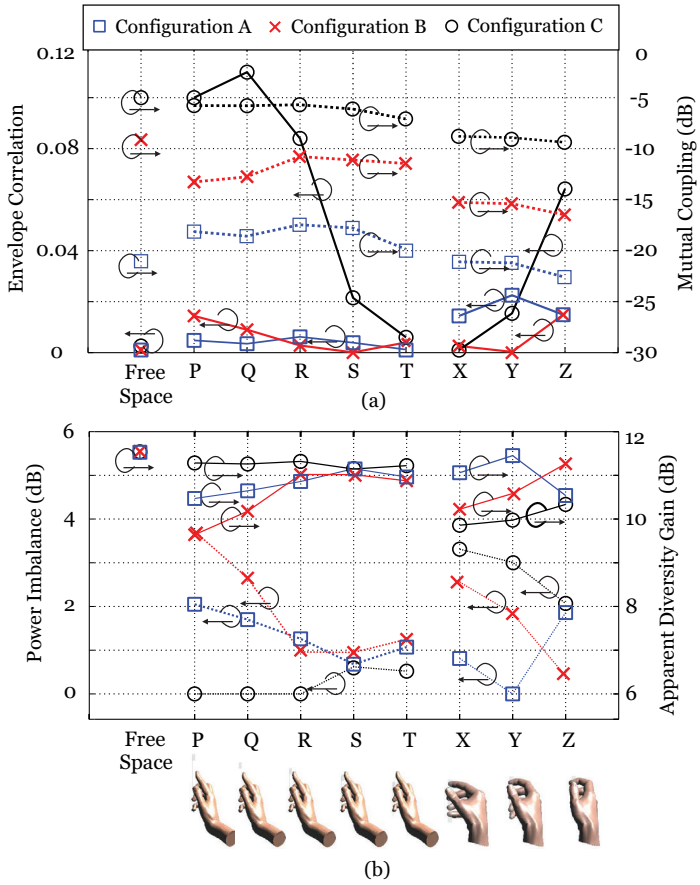

Figure 3.5. Effects of hand on dependency between (a) envelope correlation and mutual coupling, (b) power imbalance and apparent diversity gain (at 1% CDF level using the MRC technique) [**III**].

the elements.

A relative ranking from the best to worst based on the average of mutual coupling of studied antenna configurations can be obtained: 1, configuration A; 2, configuration B and 3, configuration C. The results show that no significant changes in the ranking is observed, when the mutual coupling is compared in the presence and absence of user's hand.

In general, envelope correlations are fairly close to each other and reasonably small. No relation is found between the envelope correlation and mutual coupling. However, it is of fundamental importance to obtain low mutual coupling in the absence of hand, since it typically indicates low mutual coupling also in the presence of user's hand.

Fig. 3.5(b) shows that there exist power imbalances across most of the tested hand positions, except for location P, Q and R of configuration C, and location Y of configuration A, where both elements are positioned

away from the index finger. The most significant imbalance is obtained at location P for configuration B, where the imbalance is 3.7 dB. This is because only B2 is in the close proximity of the palm, while B1 is farther away from the hand. It can be observed that a significant power imbalance and thus the *ADG* degradation occurs when the user's hand is much closer to one element than the other.

For diversity performance evaluation in a non-uniform propagation environment, a multi-antenna structure operating at 3500 MHz in the presence of one and two hands is investigated [**IV**]. The number of antenna elements is increased from two presented in [**I**] and [**III**], to four antennas. The angular power spectrum (APS) using Gaussian distribution for the elevation angle under various incident APS parameters and *XPR*s is used. The Gaussian distribution is expressed by [18]:

$$P_{\theta,\phi}(\theta) \propto \exp\left[-\frac{(\theta-\theta_0)^2}{2\sigma^2}\right], \tag{3.3}$$

where θ_0 is the peak elevation angular power spectrum (APS) at the mobile terminal for θ- polarized component, and σ controls the spread of the distribution. The APS in the ϕ- polarized component is uniformly distributed.

The multiple antenna selection scheme [89] is utilized in [**IV**]. Diversity antenna selection with use of only the best two out of four antenna elements using maximum ratio combining (MRC) technique is utilized. The technique is called generalized selection combining (GSC) [90]. For comparison, the conventional selection combining (SC) and MRC techniques using all four antennas are investigated and compared.

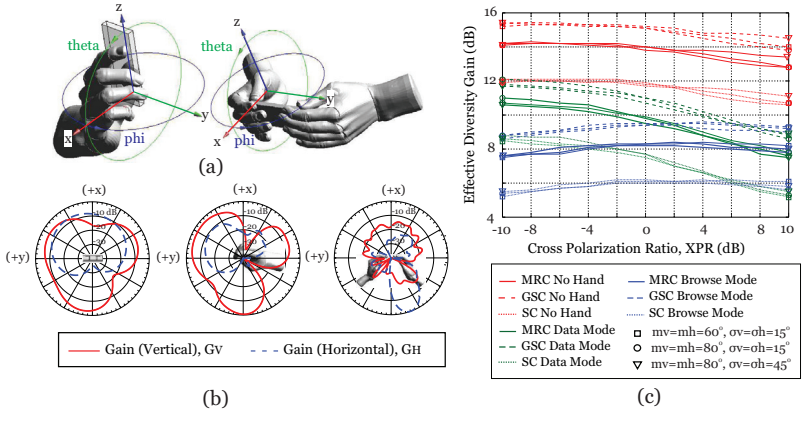

Figure 3.6. (a) Data and browsing modes with coordinates system used, (b) normalized azimuth partial gains when element 1 is excited, and (c) *EDG* versus *XPR*s, mean values and angular spreads [**IV**].

Fig. 3.6 shows that at 1% cumulative distribution function (CDF) level, the GSC (best two antennas) achieves 2 dB higher *EDG* than the SC (all four antennas), and only 1 dB less than the MRC (all four antennas) technique. It is found that the *XPR* value has important influence on *EDG*s due to the power imbalance between the partial power gain patterns (2.5). On the other hand, the effect of the incident wave parameters of the propagation environment on the *EDG* performance is almost negligible.

3.3 User effect on MIMO channel capacity

In [**VI**], MIMO channel capacity is evaluated using the same set of multi-antenna structures and hand grips as in [**III**]. The embedded patterns obtained from simulations are combined with experimental outdoor micro-cellular propagation data obtained at 2154 MHz (see Fig. 2.3(b) for details) by MEBAT. The resultant CDF of the instantaneous MIMO channel capacity of the studied multi-antenna configurations are shown in Fig. 3.7.

In this study, at median CDF level, a maximum reduction of 3.6 bit/s/Hz in MIMO channel capacity due to the user's hand is observed. The palm has the major impact on reducing MIMO channel capacity, wherein the worst use position is the one with the palm closest to the multi-antenna

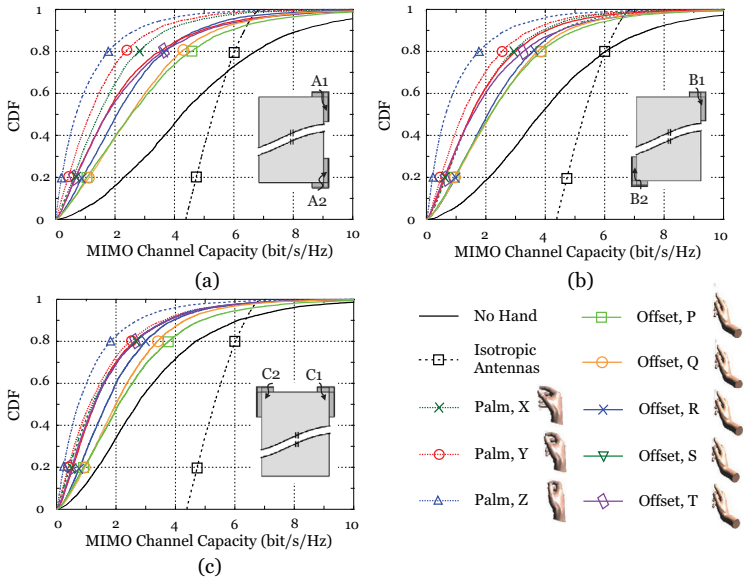

Figure 3.7. Effects of hands on MIMO channel capacity (SNR = 10 dB) for (a) configuration A, (b) configuration B and (c) configuration C [**VI**].

structure. The effect of index finger position turned out to be less significant. The proximity of the index finger to only one of the two elements results in significant power imbalance [**III**]. However, the impact of index finger position is found to be insignificant, when the MIMO channel capacity is evaluated using experimental propagation data.

It is important to note that the degradation of MIMO channel capacity largely depends on the user's hand grip. One of the possible solutions to compensate the MIMO channel capacity degradation caused by the user's hand is to employ more antennas in the same terminal. Hence, the impact of integrating antennas on MIMO channel capacity in the presence of user's hand is investigated.

3.4 Impact of incorporating antennas on MIMO channel capacity

The necessity of employing more antennas in mobile terminal when the user's hand is present was studied in [**II**]. Evaluation of multi-antenna structures operating at 3500 MHz with two- and eight-element antennas is performed. The propagation environment used in the evaluation is illustrated in Fig. 2.3(a).

For each multi-antenna configuration, the MIMO channel capacity (2.19) is computed. After that, the designed and evaluated structures are ranked according to the MIMO channel capacity[2]. Four different structures comprising of two- and eight-element antenna structures are investigated, as shown in Fig. 3.8. For fair comparison, antenna placement for all structures are fixed, and the size of the terminal chassis is kept at 100×40 mm^2.

MIMO channel capacities for different structures and grips are shown in Fig. 3.9. The MIMO channel capacity degradation due to the presence of user's hands resulted into a similar degradation for '2-CF' and '2-PIFA' structures, i.e., on an average, there is 53% and 80% reduction in the presence of one and two hands, respectively. MIMO channel capacities for '8-CF' and '8-PIFA' structures are also degraded similarly but with smaller degradation percentage, that is 38% and 65% reduction for one and two hands, respectively. On average, the MIMO channel capacity is degraded of about 45% and 75% in the presence of one and two hands, respectively.

The similar degradation of MIMO channel capacity suggests that when

[2] from the worst (most-left) to the best (most-right) multi-antenna design shown in Fig. 3.9.

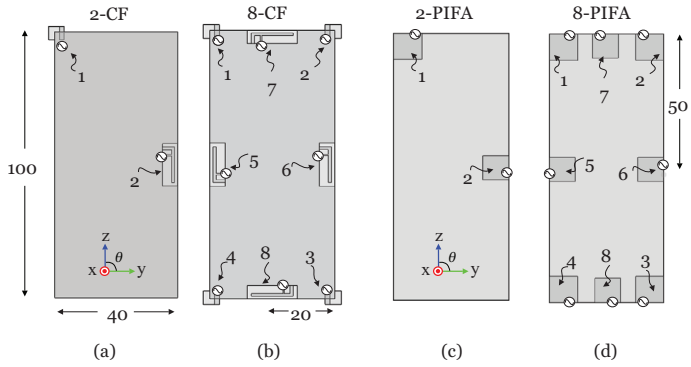

Figure 3.8. Multi-antenna under test; (a) '2-CF", (b) '8-CF", (c) '2-PIFA' and (d) '8-PIFA'. See [**II**] for the details of the antenna dimension.

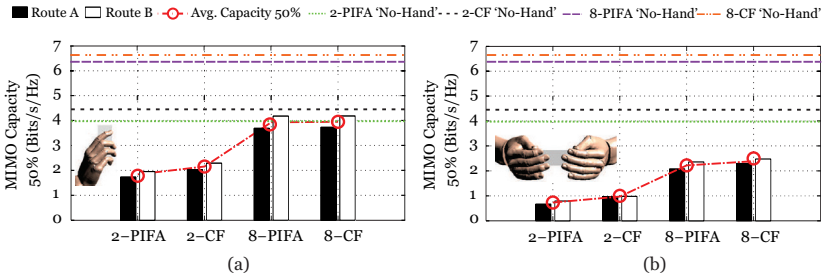

Figure 3.9. Multi-antenna performance ranking at 50% probability level for MIMO channel capacity (SNR = 10 dB); with (a) data mode and (b) browsing mode [**II**]. Route A and B represent an obstructed LOS and non LOS scenarios, respectively.

several multi-antenna structures with the same amount of antennas are compared, the one that achieved higher MIMO channel capacity in the absence of hand seems also to achieve relatively higher MIMO channel capacity in the presence of user's hand. Hence, it is important to achieve high MIMO channel capacity in the absence of hand.

In this study, it is observed that the degradation of MIMO channel capacity due to the presence of user's hand is reduced by only about 15%, when eight antennas is employed instead of two antennas. Increasing the number of antennas leads to an increase in complexity of the RF circuitry. In addition, the volume required to implement eight antennas on the terminal chassis is larger. Therefore, the improvement of MIMO channel capacity offered by incorporating more antenna elements comes at the expense of additional RF chains and volume, that are difficult to implement on the relatively small mobile terminal chassis. According to this study, it is shown that increasing the number of antennas above two may not be feasible taking into account the added complexity.

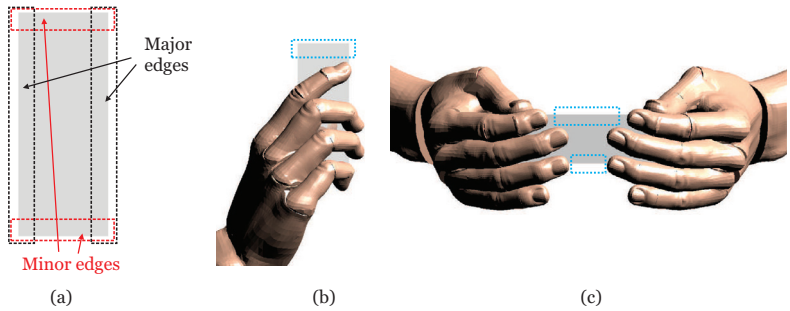

Figure 3.10. (a) Available antenna placement, and terminal chassis with user's (b) one hand, and (c) two hands. The blue dotted lines represent areas where antenna location is less obstructed with the user's hand [**II**].

3.5 Compensation of the effect of the user at an early design stage

In [**II**], antenna locations that are tolerant to the presence of user's hand are studied. It is well-known that locations near the major and minor edges of the terminal chassis are practical for antenna elements. The center portion is typically reserved for other components such as display, RF devices and integrated circuits, loudspeakers, camera, vibrators and battery [19, 32]. The available area for antenna placement is shown in Fig. 3.10(a). Based on the grips with one and two hands, the available space left for placing the antenna elements is limited as shown in Figs. 3.10(b) and 3.10(c), respectively.

In [**II**], multiple antennas are proposed to be located at the top corner and center of the terminal's major edge. These locations are selected to compensate the effect of the user's hand for both hand grips simultaneously. The performance of two- and eight-element antenna structures at the proposed locations is investigated in [**II**]. Evidently, at least one antenna is unobstructed for each user's hand grip. Regardless of mobility of the user, the unobstructed antennas resulted significant improvement in the received SNR by up to 20 dB, as compared to the obstructed antennas [91].

4. Novel multi-antenna structures and measurement techniques

As modern mobile terminals are designed to support multiple technologies such as GSM, 3G, Bluetooth, global positioning system (GPS), wireless local area network (WLAN), WiMAX, LTE, etc, the number of antennas has increased drastically [22, 92]. Major challenges related to the large number of antennas are the small volume reserved for individual antenna and mutual coupling between antennas [22]. Therefore, an efficient multi-antenna design is indeed important.

In Section 4.1, novel multi-antenna solutions comprising of two elements operating at 900 MHz UHF in [**VII**], and 3500 MHz LTE and WiMAX technology bands in [**II**] are proposed. Five- and eight-element antennas operating at 3500 MHz bands are presented in [**II**] and [**VIII**], respectively. The performance of the proposed designs are evaluated by means of diversity and MIMO performance metrics.

Potential applications based on multi-element antennas include radio direction finding (RDF) [22, 93]. Multi-antenna system of the RDF is designed to sample an incident signal in such a way that an RDF receiver and signal processing unit can estimate the direction of arrival (DoA) of the signal accurately. Therefore, obtaining unambiguous DoA estimation is desired when designing the multi-antenna structure for RDF system. Ambiguity array function can be used to characterize ambiguity level of the multi-antenna system in receiving signals. In Section 4.2, ambiguity characterization and its relation to multi-antenna locations in mobile terminals are studied [**VIII**], [**IX**].

Traditional measurement techniques cannot be used directly to characterize antenna in multipath environment. In Section 4.3, measurement techniques using anechoic and reverberation chambers are compared [**V**].

4.1 Multi-antenna structures for diversity and MIMO applications

4.1.1 Two-element antenna structure

This section focuses on techniques to reduce mutual coupling at 900 MHz band, and selection of suitable antenna type operating at 3500 MHz to achieve good MIMO performance.

Mitigation of mutual coupling at 900 MHz

Decoupling multiple antennas in small mobile terminal has gained much attention especially at the lower UHF frequencies [13, 94]. Several decoupling techniques based on the concept of characteristic wavemodes [95–97] and multi-antenna excitation methods [98, 99] are proposed.

The concept of balanced antenna and its feasibility for mobile terminals is studied in [100–102]. One of the benefits of using balanced antenna is that the coupling between the antenna and the terminal chassis is small [102]. It is useful at the lower UHF frequencies, since the radiation is mainly from the mobile terminal chassis [28, 33, 103]. Therefore, realization of a balanced antenna as one of the two radiating elements in two-element structure is introduced in [**VII**].

Fig. 4.1 illustrates the proposed balanced and unbalanced (BuB) two-element structure. The BuB comprises of a balanced antenna, i.e., electrically isolated bow-tie antenna from the terminal chassis, and a CCE at the opposite end of the terminal chassis. The reference structures with identical antenna elements are compared to the proposed BuB structure. Reference structure #1 (see Fig. 4.2(b)) comprises of two CCEs located at the opposite ends of the terminal chassis. Meanwhile, reference structure #2 (see Fig. 4.2(c)) comprises of two corner-type CCEs located at the corners of the same short edge of the terminal chassis.

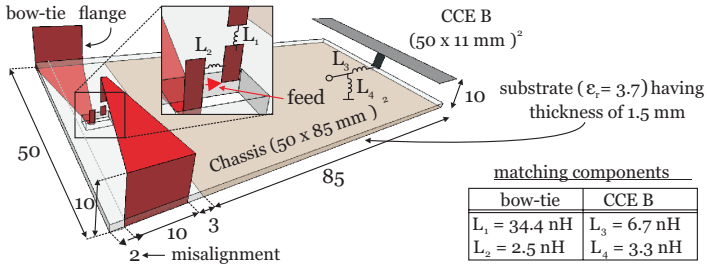

Figure 4.1. BuB two-element structure, consisting CCE and bow-tie antennas [**VII**]. Dimensions are in millimeters.

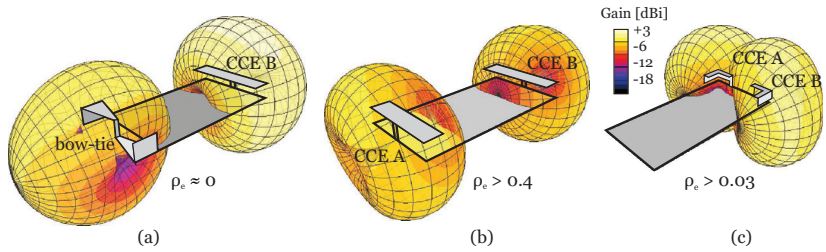

Figure 4.2. Simulated 3D embedded element patterns of (a) the BuB structure, (b) the reference #1 and (c) the reference #2 structures. The envelope correlation values are the minimum of the three evaluated environments. See Figs. 2 and 3 in [**VII**] for details of the reference antennas.

Fig. 4.2 also shows the embedded element patterns for all studied structures. Both the balanced and unbalanced antennas have embedded element pattern similar to that of a dipole antenna, as shown in Fig. 4.2(a). The omni-directional embedded element patterns are aligned orthogonal to each other, and therefore the envelope correlation is low. Identical embedded element patterns in reference structure #1 exhibits high envelope correlation, i.e., $\rho_{\mathrm{e}} > 0.4$ as shown in Fig. 4.2(b)). Fig. 4.2(c) shows that the envelope correlation of reference #2 structure is low ($\rho_{\mathrm{e}} > 0.03$). The low envelope correlation in reference #2 structure results from the exploited angle diversity.

The mutual coupling in the proposed BuB structure is -22 dB. However, the exhibited mutual coupling for reference #1 and #2 structures are -3.5 and -5.5 dB, respectively. It can be concluded that low envelope correlation does not necessarily indicate low mutual coupling.

Diversity parameters of the proposed and reference structures are listed in Table 4.1. From Table 4.1, the *EDG* of BuB structure is better than the two reference structures in all evaluated environments, with the largest difference being 6.3 dB. It is shown that the proposed BuB structure with

Table 4.1. Estimated DG Performance (at 1% CDF level) in Different Propagation Environments at 900 MHz.

Structure	**Isotropic Uniform APS**[1]				**Urban 1**[2]				**Urban 2**[3]			
	ρ_{e}	MEG_1 (dB)	MEG_2 (dB)	*ADG* / *EDG* (dB)	ρ_{e}	MEG_1 (dB)	MEG_2 (dB)	*ADG* / *EDG* (dB)	ρ_{e}	MEG_1 (dB)	MEG_2 (dB)	*ADG* / *EDG* (dB)
Ref. #1	0.406	-6.54	-6.54	10.44 / 7.12	0.787	-9.22	-5.88	6.78 / 3.46	0.817	-6.19	-4.26	7.51 / 4.19
Ref. #2	0.028	-4.70	-4.70	11.44 / 9.89	0.083	-6.41	-3.12	9.69 / 8.14	0.405	-3.88	-3.33	10.16 / 8.61
BuB	0.000	-3.13	-3.19	11.47 / 11.41	0.112	-2.83	-5.69	9.83 / 9.77	0.002	-4.32	-2.25	10.47 / 10.41

Apparent diversity gain, *ADG* using maximum ratio combining (MRC) technique

MEG_1 refers to the bow-tie or CCE A

MEG_2 refers to the CCE B

[1] Isotropic uniform: *XPR* = 0 dB, $m_{\mathrm{v}} = m_{\mathrm{h}} = 0^{\circ}$, $\sigma_{\mathrm{v}} = \sigma_{\mathrm{h}} = \infty$

Scenario parameters in azimuth plane are uniform, and elevation plane are the following (Gaussian) [44]:

[2] Urban 1: Tokyo, the Ningyo-cho route: *XPR* = 5.1 dB, $m_{\mathrm{v}} = 19^{\circ}$, $\sigma_{\mathrm{v}} = 20^{\circ}$, $m_{\mathrm{h}} = 32^{\circ}$, $\sigma_{\mathrm{h}} = 64^{\circ}$

[3] Urban 2: Tokyo, the Kabuto-cho route: *XPR* = 6.8 dB, $m_{\mathrm{v}} = 20^{\circ}$, $\sigma_{\mathrm{v}} = 42^{\circ}$, $m_{\mathrm{h}} = 50^{\circ}$, $\sigma_{\mathrm{h}} = 90^{\circ}$

low mutual coupling and good *EDG* performance seems to be a promising solution for diversity applications at 900 MHz.

Utilization of antenna current localization at 3500 MHz

As frequency increases, the physical dimensions of the antennas decreases and inter-element spacing increases. At higher frequencies, space limitation is not so severe and contribution of the terminal chassis is not significant. Single and multiple antennas are designed using PIFA, monopole, IFA and CCE in 3400-3600 MHz band [104–107]. In [**II**], PIFA, IFA and CCE antennas are investigated. The current distribution on the terminal chassis is investigated to incorporate two or more antennas with low mutual coupling on the same terminal [96].

Fig. 4.3 shows normalized (maximum value equals to unity) current distributions of PIFA, IFA and CCE antennas on the terminal chassis. It is observed that the current of the PIFA is less localized than that of the IFA and CCE. The localized chassis current of the IFA and CCE antennas show that the radiation depends less on the terminal chassis.

In [**II**], only two extreme cases of antennas with 1) localized and 2) less localized chassis current distributions are investigated. A combination of antennas with localized chassis current distribution is proposed by using CCE and IFA. Identical less localized PIFAs are designed as a reference structure. Both structures referred to as '2-CF' and '2-PIFA' are shown in Figs. 3.8(a) and 3.8(c), respectively. Additionally, computational '2-ISO'

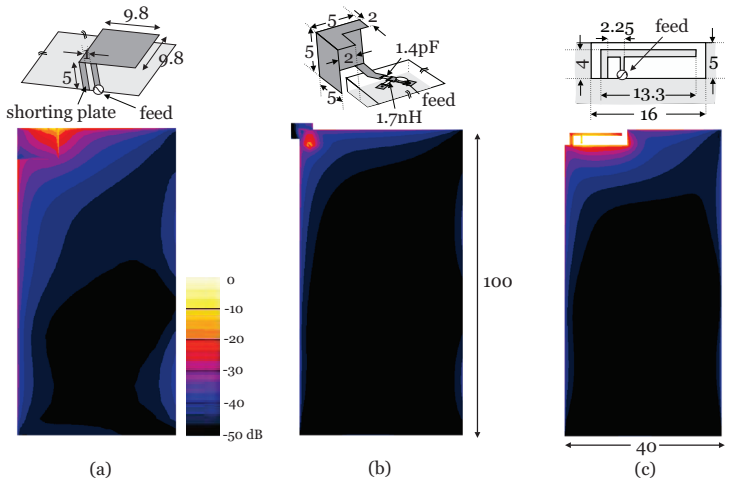

Figure 4.3. Antenna geometries and corresponding normalized magnitude of current distributions for (a) PIFA, (b) CCE and (c) IFA. All dimensions are in millimeters [**II**].

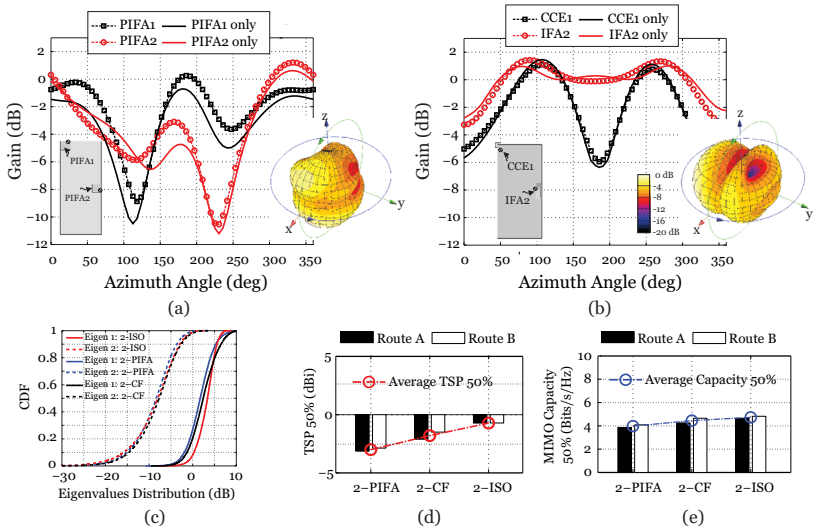

Figure 4.4. Azimuthal (xy-plane) gain pattern and corresponding combined radiation pattern for (a) '2-PIFA', (b) '2-CF', (c) eigenvalue distributions for 2×2 MIMO system in Route A, and multi-antenna performance ranking at 50% probability level for (d) *TSP* and (e) MIMO channel capacity (SNR = 10 dB). Details of the measurement routes can be found in [**II**].

structure comprising of two isotropic antennas is designed for power normalization in the evaluation of MIMO channel capacity (2.20). The locations of the '2-ISO' antenna elements are the same as those of the '2-PIFA' and '2-CF' structures.

In the 3400-3600 MHz band, the mutual coupling of '2-CF' and '2-PIFA' structures are relatively small, i.e., better than -16.5 dB due to the electrically large antenna separation in the structures. The impact of localized current distribution on the embedded element pattern is studied. Figs. 4.4(a) and 4.4(b) show the gain of each antenna element in the presence and absence of the second antenna element. It shows that both the CCE and IFA in the '2-CF' structure maintain their embedded element patterns when the second antenna element is added on the same terminal chassis. However, the embedded element pattern of the '2-PIFA' structure changes more when the second element is added. It indicates higher tolerance of the current localized antennas to the presence of other antennas on the same chassis.

The normalized combined radiation pattern for the studied structures are also shown in Figs. 4.4(a) and 4.4(b), respectively. The gains are normalized to the highest gain among the antenna elements, with total input power of 1 W distributed amongst all antennas. In the '2-CF' structure, the beam-width of the combined radiation pattern is increased and thus

yields a more isotropic pattern than the '2-PIFA' structure. When the current is localized, it seems to be easier to exploit pattern, spatial and angle diversities independently.

The eigenvalue distribution obtained with the studied structures is shown in Fig. 4.4(c). It shows that the difference between the first and second eigenvalues for '2-ISO', '2-PIFA' and '2-CF' are similar. This suggests that different types of antenna with the same number of antenna elements do not seem to affect the eigenvalue distribution of a MIMO system.

Figs. 4.4(d) and 4.4(e) show that the transferred signal power, *TSP* (2.21) level of the multi-antenna system plays an essential role in achieving high MIMO channel capacity. At 50% probability level, the '2-CF' structure achieves 17% higher MIMO channel capacity than the '2-PIFA', and 35% less than the isotropic structure. It can be concluded that the combined radiation pattern with more omnidirectional pattern has improved the *TSP* and hence improved the MIMO channel capacity.

4.1.2 Five-element antenna structure

A five-element antenna comprising of IFAs operating at 3500 MHz is presented in [**VIII**]. The IFAs are integrated along the edges of the upper ground plane of a clamshell type mobile terminal. The antennas are located on the upper ground plane to reduce the effect of the user, whose hand is typically gripping the bottom part of the mobile terminal either in the data or browsing mode. The location and orientation of the antennas are selected such that the mutual coupling is low, i.e., less than -10 dB within 3400-3600 MHz band. For simplicity, additional structures to mitigate mutual coupling between antenna elements is avoided, such as de-

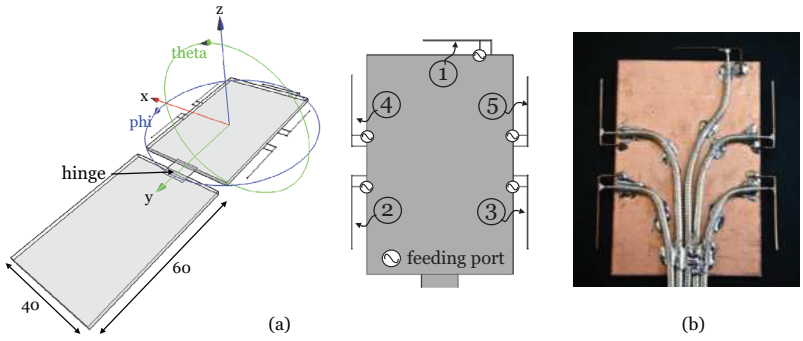

Figure 4.5. Five-element IFA array structure used in (a) simulation and (b) measurement. All dimensions are in millimeter. See [**VIII**] for details of the antenna dimensions.

Table 4.2. Mutual Coupling, Envelope Correlation and Apparent Diversity Gain (at 1% CDF level) at 3500 MHz

Ports	Sim. / Meas. Mutual Coupling (dB)	Envelope Correlation, ρ_e	SC *ADG* (dB)
1-2	-18.9 / -18.8	0.2	9.8
1-3	-20.4 / -19.1	0.1	10.0
1-4	-6.4 / -6.4	0.2	9.8
1-5	-9.8 / -10.3	0.2	9.8
2-3	-9.7 / -8.6	0.1	9.9
2-4	-10 / -11.6	0.2	9.8
2-5	-17.4 / -17.8	0.2	9.8
3-4	-18.3 / -18.1	0.2	9.9
3-5	-9.3 / -14.5	0.2	9.9
4-5	-20.3 / -15.6	0.2	9.8

SC *ADG* = Apparent diversity gain using selection combining technique

coupling network [108, 109], defected ground plane [110, 111] or parasitic element [112]. Fig. 4.5 shows the proposed structure and the fabricated prototype.

The IFAs are first designed at their predefined locations. IFA_2–IFA_4 and IFA_3–IFA_5 configurations are oriented such that the ground pins are next to each other. Separation between IFA_1 and IFA_4 is increased so that mutual coupling between IFA_1 and IFA_5 is less than -10 dB. However, high mutual coupling of -6.4 dB is exhibited for the IFA_1–IFA_4 pair.

Table 4.2 lists simulation and measurement results of mutual coupling between antenna elements. The diversity parameters comprising of envelope correlation, ρ_e and apparent diversity gain, *ADG* under selection combining technique are also listed. The discrepancies between simulation and measurement results were mainly due to the effect of five measurement cables, and the inaccuracies in the manufacturing of the prototype. Results show that all antenna ports exhibited a good performance with low envelope correlation and high *ADG*.

4.1.3 Eight-element antenna structure

In [**II**], an eight-element antenna structure consisting of four CCEs at every chassis corner, and four differently oriented IFAs around the chassis is proposed. The structure referred to as '8-CF' is designed to provide the largest MIMO channel capacity among the studied multi-antenna structures in [**II**]. The size of the CCEs and the IFAs are the same as in the '2-CF' proposed in Section 4.4. Eight-element PIFAs referred to as '8-

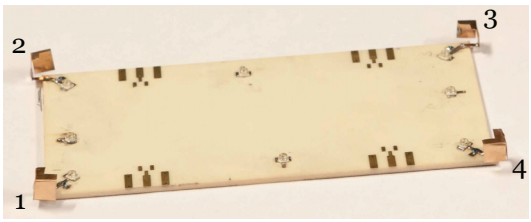

Port	L_{shunt}
1	1.5 nH
2	2.3 nH
3	1.5 nH
4	2.3 nH

(a)

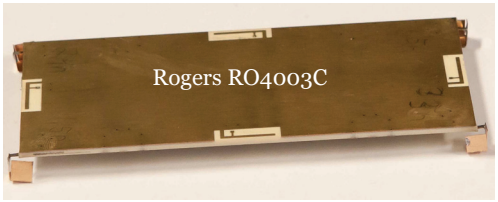

(b)

Figure 4.6. The '8-CF' prototype from (a) top view, with lumped components used to match associated CCE ports and (b) rear view. See [**II**] for details of the antenna dimensions.

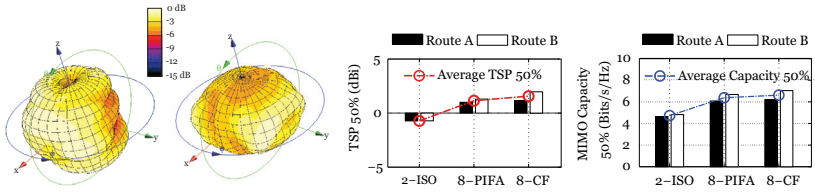

(a) (b) (c) (d)

Figure 4.7. Combined radiation pattern for (a) '8-PIFA', (b) '8-CF' and multi-antenna performance ranking at 50% probability level for (c) *TSP*, (d) MIMO channel capacity (SNR = 10 dB). Details of the measurement routes can be found in [**II**].

PIFA' is designed as a reference structure (see Fig. 3.8(d)). The prototype of the '8-CF' structure is shown in Fig. 4.6.

In the 3400-3600 MHz band, the measured impedance matching is -8 dB with the strongest mutual coupling being -10 dB. The average mutual coupling over all antennas in the frequency band is -19.7 and -21.1 dB for simulated and measured results, respectively. The measured embedded element and total embedded element efficiencies in the frequency band are between -2.1 to -1.9 dB (61 - 64 %) and -2.6 dB to -2.3 dB (55 - 59 %), respectively.

Figs. 4.7(a) and 4.7(b) show the combined radiation pattern for '8-PIFA' and '8-CF' structures, respectively. The combined radiation pattern of '8-CF' is more isotropic than that of the '8-CF' structure. Figs. 4.7(c) and 4.7(b) show the evaluated *TSP*s and MIMO channel capacity for '8-PIFA' and '8-CF' structures, respectively. At 50% probability level, the *TSP*s of

'8-PIFA' and '8-CF" structures are positive values with difference of 1.8 dB and 2.3 dB respectively as compared to the '2-ISO' structure.

The calculated *EDG* performance using maximum ratio combining (MRC) technique at 1% CDF level (2.17) for '8-CF' is 20.1 dB. The propagation environment is modelled as an isotropic uniform one. For the same number of uncorrelated isotropic antennas, the calculated *EDG* is 24.6 dB. The 4.5 dB difference is due to small *MEG*, since envelope correlations ρ_{e} (2.11) between elements are very small. Reduction in the *MEG* is largely due to the constructive impact of the mutual couplings from all eight antennas. The envelope correlation meets the MIMO LTE requirements for spatial diversity, i.e., $\rho_{\mathrm{e}} \leq 0.3$ [49].

It is shown that if a multi-antenna structure is designed carefully; fitting a compact mobile terminal with as much as eight antennas can increase the MIMO channel capacity by about 65% compared to two-element antennas, at the expense of increased structure complexity.

4.2 Multi-antenna structures for radio direction finding

Radio direction finding (RDF) has been introduced as one possible feature in mobile terminals [22, 93]. In direction-of-arrival (DoA) estimation, mutual coupling between the antenna elements is often considered as an undesired effect, which contributes to a significant degradation of the estimation accuracy if not fully taken into account by the estimation algorithm [113–116].

In an RDF system, DoA estimation algorithm should be able to discriminate DoAs ambiguously. This ability can be determined by simply scanning through all DoAs of interest, and is computed using the expression [117], [**VIII**], [**IX**]:

$$\left|\chi_{ij}\left(\phi_i,\phi_j\right)\right| = \left|\frac{\mathbf{E}_{\phi,\theta}\left(\pi/2,\phi_i\right)^{\mathrm{H}}\mathbf{E}_{\phi,\theta}\left(\pi/2,\phi_j\right)}{\left\|\mathbf{E}_{\phi,\theta}\left(\pi/2,\phi_i\right)\cdot\mathbf{E}_{\phi,\theta}\left(\pi/2,\phi_j\right)\right\|}\right|, \tag{4.1}$$

where $\mathbf{E}_{\phi,\theta}\left(\pi/2,\phi\right)$ is an electric field vector in the azimuth plane, i.e., $\theta = \pi/2$. $(\cdot)^{\mathrm{H}}$ denotes as complex transpose and $\|\cdot\|$ represents the Euclidean norm of the vector. The array ambiguity function (4.1) ranges between 0 and 1, which correspond to very good orthogonality and collinearity, respectively. Fig. 4.8(a) shows perfect orthogonality of the multi-antenna response to different angles. It is characterized from an infinitely large multi-antenna aperture. Fig. 4.8(b) represent the corresponding ambiguity array function of a finite multi-antenna aperture. Typically, such a

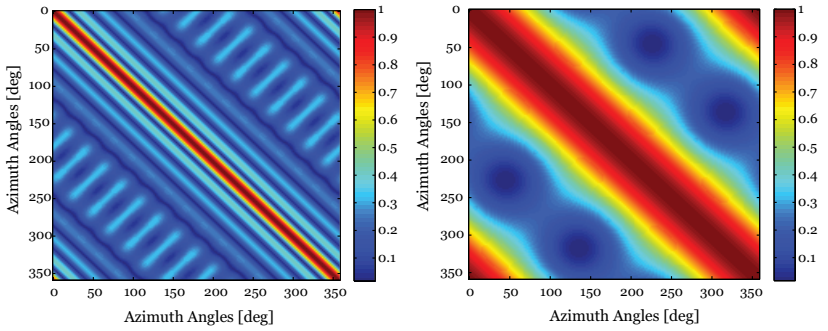

Figure 4.8. Array ambiguity functions of a uniform circular array composed of (a) 16 Hertzian dipoles within a diameter of 200 mm and (b) 4 Hertzian dipoles within a diameter of 30 mm. The operating frequency is assumed to be 3500 MHz [**IX**].

diagonal region is inversely proportional to the aperture size of the multi-antenna system. In addition, the array ambiguity function may be composed of out-of-diagonal-region peaks. These are commonly due to the configuration of the antennas, radiation pattern of the antenna elements, mutual coupling, terminal chassis reflections, etc [**IX**]. When designing a multi-antenna system, one is typically interested in the array ambiguity function shown in Fig. 4.8(a).

Ambiguity peaks indicate that two (or more) possible DoAs cannot be separated. The array ambiguity measures the correlation of the steering electric field vectors which should be as small as possible, meeting the criterion of $|\chi_{ij}(\phi_i, \phi_j)| \leq 0.7$. The condition is similar to the requirement for low envelope correlation in diversity and MIMO applications [4, 18].

In [**VIII**], a feasibility study for RDF application using a five-element IFA on a clamshell-type terminal chassis (see Section 4.1.2) is presented. In [**IX**], ambiguities of four-element antennas at different locations exhibiting different mutual couplings are investigated. In this [**VIII**] and [**IX**], the ambiguities are evaluated in the case of receiving a ϕ-polarized incident signal in the azimuth (x-y plane) with the DoA spanning 360°. Fig. 4.9(a) represents the coordinate system used for the incident signal. Fig. 4.9(b) to 4.9(f) show the array ambiguity functions for all the studied structures. The corresponding combined electric field pattern for the studied structures are also shown. The combined electric field pattern is normalized to the highest electric field among the antenna elements.

Fig. 4.9(b) shows antenna elements that are located at the edges of the chassis, wherein the combined electric field pattern is more directive due

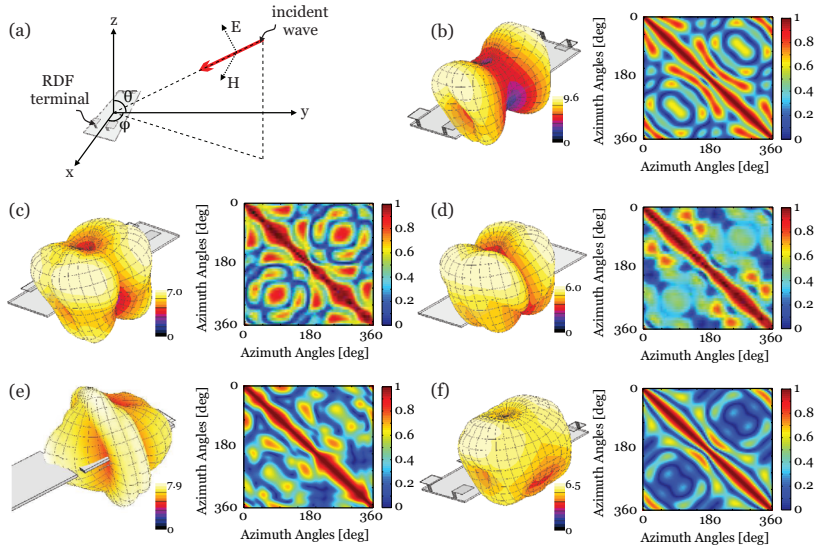

Figure 4.9. (a) Spherical coordinate used in description of incident wave, and the array ambiguity functions in ϕ-polarization with corresponding combined electric field pattern (V/m) for four-element antenna structure of (b) model A, (c) model B, (d) and model C [**IX**], (d) five-element antenna structure [**VIII**] and (e) eight-element antenna structure [**IX**]. See [**VIII**] and [**IX**] for details of the antennas.

to large antenna separation along the major chassis edges. The average mutual coupling is -18 dB, with maximum antenna spacing of 0.97λ. Figs. 4.9(c) and 4.9(d) show the ambiguity array functions when the elements are placed closer to the center of the terminal chassis. The average mutual coupling in model B and C increases from -32 to -8 dB, when the maximum spacing between elements in model B and C are 0.75λ and 0.40λ, respectively. The beam-width of the combined electric field patterns (see Figs. 4.9(c) and 4.9(d)) increases resulting in more an omnidirectional pattern in the azimuth plane, as compared to the combined electric field pattern of model A shown in Fig. 4.9(b). The combined electric field pattern and associated ambiguity array function for larger number of incorporated antenna elements, that is with five-element [**VIII**] and eight-element antenna array [**IX**] are also shown in Figs. 4.9(e) and 4.9(f), respectively.

In the studied structures, the multi-antenna structure patterns are less ambiguous (peaks of ambiguity array are less than 0.7) when the inter-element spacing between antennas decreases. The more isotropic pattern seems to reduce ambiguity of the multi-antenna structure. Non-uniform spacing between the antenna elements has improved the reduction of am-

biguity [118], and it is proven to be feasible for mobile terminals [**VIII**].

The combined electric field pattern is used for the first time as a tool to provide insights on the ambiguity array function of a multi-antenna system. It is important to characterize the ambiguity of multi-antenna structures in mobile terminals at the early design stages. This provide a motivation for DoA estimation algorithms when the design of multi-antenna structure is characterized to be unambiguous.

4.3 Comparison of anechoic and reverberation chamber measurement techniques

Antenna performance in a line-of-sight (LOS) environment can be characterized with traditional methods, such as spherical near-field measurement technique in an anechoic chamber. However, traditional methods cannot be used to characterize antenna in multipath environment. Hence, measurement techniques for small antennas in multipath environment are needed. A reverberation chamber emulating multipath environment can be used to measure the efficiency, diversity and MIMO parameters [36]. Measurement campaigns at Technical University of Denmark and Chalmers University of Technology are performed to compare two measurement techniques for over-the-air (OTA) diversity and MIMO terminal

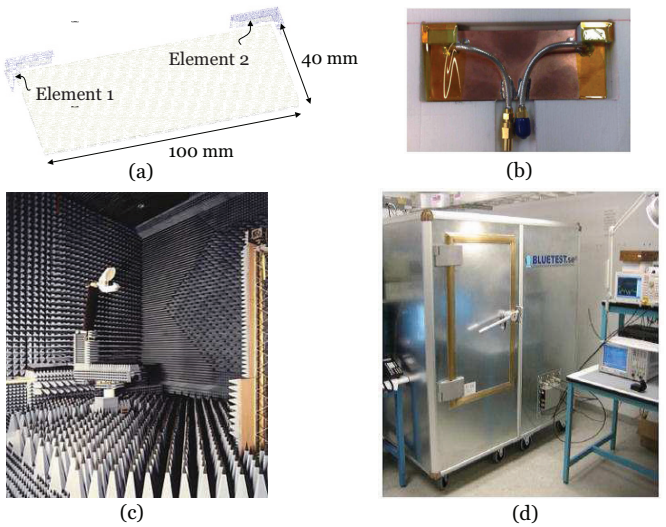

Figure 4.10. (a) Simulation model, (b) fabricated prototype, and measurements performed in (c) anechoic chamber by spherical near-field technique at Technical University of Denmark, and (d) reverberation chamber at Chalmers University of Technology. See [**V**] for details of the antenna dimension.

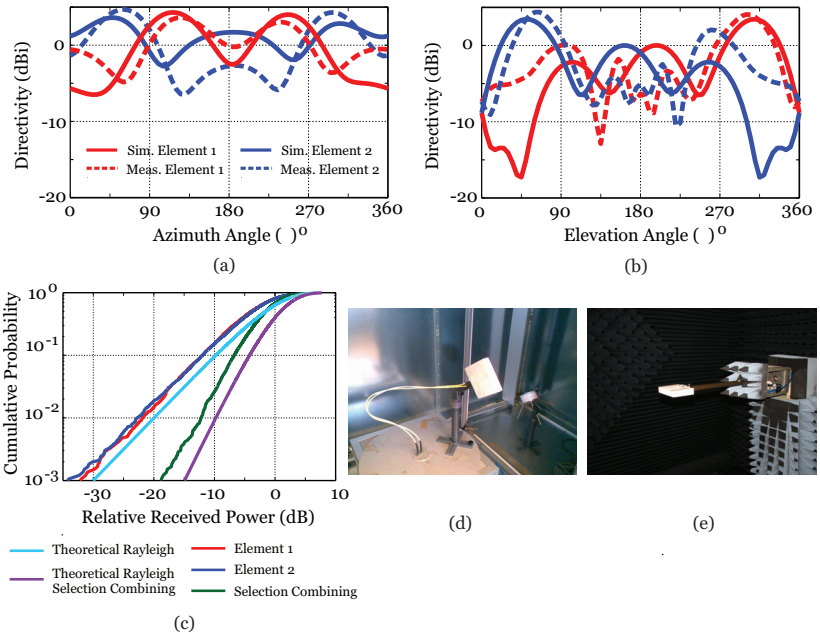

Figure 4.11. Embedded element patterns for associated antenna element in (a) azimuth, (b) elevation angle, (c) measured CDF in reverberation chamber, and measurement setups in (d) reverberation and (e) anechoic chambers [**V**].

testing.

In [**V**], diversity performance of a two-element mobile terminal structure presented in [**III**] is analyzed in terms of envelope correlation, apparent and effective diversity gain. Fig. 4.10 shows different measurement techniques at anechoic and reverberation chambers. The antenna structure is simulated using a finite-difference time-domain (FDTD) -based commercial electromagnetic simulator to compare with the measurement results. A reverberation chamber can measure diversity parameters directly whereas in the anechoic chamber, the embedded element patterns are measured first and then the envelope correlation (2.11) with the APS of isotropic uniform environment is calculated. Finally, the *ADG* at 1% CDF level can be approximated by [119]:

$$ADG = 10.48\sqrt{1-\rho_e}. \tag{4.2}$$

Figs. 4.11(a) and 4.11(b) show the directivity of the embedded element patterns in azimuth and elevation planes, respectively. It indicates that embedded element patterns for associated antenna elements are in a good agreement with the FDTD simulation. The measured CDF in the reverberation chamber is shown in Fig. 4.11(c).

Table 4.3. Diversity Gains by Different Methods

Performance Metrics	**FDTD**[1]	**SNF**[2]	**RC**[3]
Envelope Correlation	0.0034	0.0017	0.0299
SC *ADG*[4]	10.2 from ρ_e	10.2 from ρ_e	10.1/9.4 from ρ_e / CDF
SC *EDG*[5]	9.7	7.8	8.0/7.3 from ρ_e / CDF

[1] FDTD = Simulation using FDTD.

[2] SNF = Measurement using spherical near-field method.

[3] RC = Measurement in reverberation chamber.

[4] SC *ADG* = Apparent diversity gain using selection combining.

[5] SC *EDG* = Effective diversity gain using selection combining.

Table 4.3 lists diversity parameters using different measurement techniques. Results of the simulated and measured envelope correlations from both techniques agree well with each other. The *ADG*s (4.2) are almost identical for the three cases, i.e., FDTD simulation, anechoic chamber and reverberation chamber, when they are estimated from the envelope correlation (2.11). There is a discrepancy of 0.8 dB between the measured results in the anechoic and reverberation chambers, when the *ADG* is estimated from the 1% level of the measured CDF curves. This error can be attributed to an uncertainty of the measured CDF at low levels.

5. Summary of the publications

[I] Influence of the user's hand on mutual coupling of dual-antenna structures on mobile terminal

The influence of some specific user's hand grips on the mutual coupling of two-element mobile antennas operating at 900, 2000, 3500 and 5300 MHz are investigated. Depending on the hand and index finger locations, up to 10 dB variations in mutual coupling are observed. The Poynting vector distribution provides insight on the behaviour of the mutual coupling in two-element structures with the presence of user's hand.

[II] Design and measurement -based evaluation of multi-antenna mobile terminals for LTE 3500 MHz band

Two- and eight-element antennas operating at 3500 MHz are designed. An isotropic radiation pattern that can receive incoming signals from arbitrary directions can be obtained by combining the radiation patterns from multiple antennas with localized chassis current distribution. The designs are shown to achieve higher MIMO channel capacity than multiple antennas with less localized current distribution. The results show that antenna type, geometry, current distribution on the terminal chassis and radiation pattern of individual antenna element must be jointly considered in order to optimize the performance of a multi-antenna structure for mobile terminal. In this paper, it is observed that the degradation of MIMO channel capacity due to the presence of user's hand is reduced by only about 15%, when eight antennas is employed instead of two antennas.

[III] Coupling element –based dual-antenna structures with hand effects

Performance of coupling element -based dual-antenna structures in the presence of hand is presented. Two types of significant hand effects; vertical position of hand along terminal chassis, and distance between palm and terminal chassis are varied. The results show that in isotropic uniform environment, the impact of power imbalance on diversity gain is high when index finger is much closer to one antenna element than the other.

[IV] Multi-antenna mobile terminal diversity performance in proximity to human hands under different propagation environment conditions

Multiple antenna selection is utilized to improve the diversity performance of four-element antennas in the presence of user's hand. The structure operating at 3500 MHz is investigated in a non-uniform environment. From available four antenna elements, it is found that by using two antennas with maximum ratio combining (MRC) technique, the effective diversity gain, *EDG* is only 1 dB less than that obtained using MRC with four antennas. The results show that the cross polarization ratio of the propagation environment has important influence on *EDG*s due to imbalance between the gain patterns. In the studied cases, the effect of the incident wave parameters of the propagation environment on the *EDG* performance is almost negligible.

[V] On diversity performance of two-element coupling element based antenna structure for mobile terminal

Diversity performance of a two-element coupling element -based antenna structure presented in [**III**] is measured. Performance metrics such as envelope correlation, apparent and effective diversity gains are evaluated using two measurement techniques. The measurement techniques emulate different propagation environments, 1) ideal line-of-sight environment using spherical near-field technique in anechoic chamber and 2) isotropic, i.e., statistically uniform environment inside reverberation chamber. The values of envelope correlation agree well with each other,

and the results of diversity gains are consistent when they are estimated from the envelope correlation. Discrepancy of 0.8 dB is obtained when the diversity gain is estimated from the 1% level of the measured CDF curves.

[VI] Site-specific evaluation of a MIMO channel capacity for multi-antenna mobile terminals in proximity to a human hand

The studied multi-antenna mobile terminal presented in [**III**] are evaluated with a measured propagation data, specifically in an outdoor micro-cellular environment. The hand grip is varied in terms of vertical position of hand along terminal chassis, and distance between palm and terminal chassis. The results show that at the median MIMO channel capacity, a maximum reduction of 3.6 bit/s/Hz is observed when the palm is in close proximity to the multi-antenna mobile terminal, compared to that of in free space. The MIMO channel capacity reductions are significant when all multi-antenna elements are in close proximity to the palm, compared to when only index finger is in proximity to one of the elements.

[VII] Isolation improvement method for mobile terminal antennas at lower UHF band

A novel method to improve the isolation between two antenna elements at the 900 MHz UHF band is presented. The two-element antenna structure comprises of balanced antenna, that is electrically isolated from the mobile terminal chassis, and a capacitive coupling element (CCE) antenna. The mutual coupling of the proposed structure is -22 dB. The structure is shown to provide very small envelope correlation and good diversity performance when evaluated in both uniform and non-uniform environments.

[VIII] Five-element inverted-F antenna array for MIMO communications and radio direction finding on mobile terminal

A five-element IFA array structure operating at 3500 MHz is proposed for both MIMO and radio direction finding (RDF) applications. The antenna array is tuned to have acceptable mutual coupling between antennas. The structure is shown to exhibit envelope correlation and ambiguity lower

than 0.7. A prototype is fabricated and good agreement between numerical simulation and experimental results is observed.

[IX] Ambiguity analysis of isolation-based multi-antenna structures on mobile terminal

Ambiguities for different isolation-based multi-antenna configurations are studied. The study is conducted by taking into account the effects of antenna isolation, mutual coupling between terminal chassis and antenna element, and mutual coupling among antenna elements. The results show that on the same size of the terminal chassis, a non-ambiguous multi-antenna structure can be exploited by locating antennas close to each other.

6. Conclusions

This thesis contributes to the advancement in design of efficient multi-antenna systems in compact mobile terminals. Different multi-antenna structures are studied, covering a wide range of frequency bands and locations on the terminal chassis. The effect of the user's hand with different grips is also studied. In diversity and MIMO performance evaluation, the studied antennas are arbitrarily oriented to mimic realistic usage scenarios.

The performance of a mobile terminal with multi-antenna structures depends on the propagation environment in which it operates [**II**], [**III**], [**VI**]. A uniform environment is often assumed in performance evaluation, but measured propagation data offers more reliable basis for the evaluation. In the uniform environment, antenna orientation does not matter. In author's opinion, an antenna should be evaluated both in uniform and non-uniform environments for accurate performance prediction.

The effects of user's hand on MIMO channel capacity was studied in two cases [**II**]. In one case, the mobile terminal was incorporated with two antennas, and in the other case eight antennas were used. It was found that the degradation of MIMO channel capacity due to the presence of user's hand is slightly reduced, when eight antennas is employed instead of two antennas. Drawbacks are increased complexity in switching and combining circuitries, and increased total volume of the antennas. Multiple antenna selection is one of possible solutions to reduce the complexity of the structure [**IV**], [15]. In general, efficient antenna solutions that perform well in the presence and absence of user's hand are always desired. In author's opinion, optimization and realization of antenna decoupling techniques should be done when the terminal is in the presence of user's hand. Formerly, the optimization of antenna decoupling technique in mobile terminals is often performed without the presence of

user [11, 46, 88, 97, 110, 111, 120, 121].

Localization using radio direction finding (RDF) is a possible future application in mobile terminals. The feasibility study on RDF in a mobile terminal is reported in [**VIII**] and [**IX**]. It was shown that by selecting suitable locations of the antenna elements, a multi-antenna structure with reduced ambiguity can be obtained. Non-ambiguous antenna structures facilitate the estimation of direction of arrival for RDF applications. In general, traditional performance metrics used for communication systems is also applicable to multiple antennas for RDF applications [**VIII**]. Therefore, multiple antennas for diversity, MIMO and RDF applications face the same challenges. Antennas need to be small, provide good impedance matching, low mutual coupling and envelope correlation between antennas, high radiation efficiency and be tolerant to the user.

The usage of multi-antenna structures in compact mobile terminals enables many interesting research topics in the future. Adaptability of the antennas to propagation environment is one example of such a research topic. For instance, a reconfigurable antenna can adapt its radiation properties and impedance according to the propagation environment and user interaction. Another research area could be the usage of meta-material based multi-antenna systems. Meta-material can provide small antenna size, high isolation and improved MIMO performance [122]. Apart from the mentioned topics, future work should also consider the availability and current trends of advanced signal processing and circuit design techniques. Thus, many interesting challenges are waiting to be addressed in the near future.

Bibliography

[1] E. Dahlman, S. Parkvall, J. Skold, and P. Beming, *3G Evolution: HSPA and LTE for Mobile Broadband*. Academic Press, Elsevier, 2008.

[2] E. Dahlman, S. Parkvall, and J. Skold, *4G LTE/LTE- advanced for mobile broadband*. Academic Press, Elsevier, 2011.

[3] Q. Li, X. Lin, J. Zhang, and W. Roh, "Advancement of MIMO technology in WiMAX: from IEEE 802.16d/e/j to 802.16m," *IEEE Commun. Mag.*, vol. 47, no. 6, pp. 100–107, June 2009.

[4] R. Vaughan and J. Andersen, "Antenna diversity in mobile communications," *IEEE Trans. Veh. Technol.*, vol. 36, no. 4, pp. 149–172, Nov. 1987.

[5] G. J. Foschini and M. J. Gans, "On limits of wireless communications in a fading environment when using multiple antennas," *Wireless Pers. Commun.*, vol. 6, no. 3, pp. 311–335, Mar. 1998.

[6] S. Anderson, B. Hagerman, H. Dam, U. Forssen, J. Karlsson, F. Kronestedt, S. Mazur, and K. Molnar, "Adaptive antennas for GSM and TDMA systems," *IEEE Pers. Commun.*, vol. 6, no. 3, pp. 74–86, June 1999.

[7] M. Jensen and J. Wallace, "A review of antennas and propagation for MIMO wireless communications," *IEEE Trans. Antennas Propag.*, vol. 52, no. 11, pp. 2810–2824, Nov. 2004.

[8] B. Green and M. Jensen, "Diversity performance of dual-antenna handsets near operator tissue," *IEEE Trans. Antennas Propag.*, vol. 48, no. 7, pp. 1017–1024, July 2000.

[9] K. Ogawa and T. Matsuyoshi, "An analysis of the performance of a handset diversity antenna influenced by head, hand, and shoulder effects at 900 mhz .I. effective gain characteristics," *IEEE Trans. Veh. Technol.*, vol. 50, no. 3, pp. 830–844, May 2001.

[10] K. Ogawa, T. Matsuyoshi, and K. Monma, "An analysis of the performance of a handset diversity antenna influenced by head, hand, and shoulder effects at 900 mhz .II. correlation characteristics," *IEEE Trans. Veh. Technol.*, vol. 50, no. 3, pp. 845–853, May 2001.

[11] M. Karaboikis, V. Papamichael, G. Tsachtsiris, C. Soras, and V. Makios, "Integrating compact printed antennas onto small diversity/MIMO terminals," *IEEE Trans. Antennas Propag.*, vol. 56, no. 7, pp. 2067–2078, July 2008.

[12] B. K. Lau and J. Andersen, "Unleashing multiple antenna systems in compact terminal devices," in *IEEE Int. Workshop Antenna Technol.*, Mar. 2009, pp. 1–4.

[13] V. Plicanic, B. K. Lau, A. Derneryd, and Z. Ying, "Actual diversity performance of a multiband diversity antenna with hand and head effects," *IEEE Trans. Antennas Propag.*, vol. 57, no. 5, pp. 1547–1556, May 2009.

[14] C. Luxey and D. Manteuffel, "Highly-efficient multiple antenna-systems for small MIMO devices," in *IEEE Int. Workshop Antenna Technol.*, Mar. 2010, pp. 1–6.

[15] F. Harrysson, J. Medbo, A. Molisch, A. Johansson, and F. Tufvesson, "Efficient experimental evaluation of a MIMO handset with user influence," *IEEE Trans. Wireless Commun.*, vol. 9, no. 2, pp. 853–863, Feb. 2010.

[16] F. Harrysson, A. Derneryd, and F. Tufvesson, "Evaluation of user hand and body impact on multiple antenna handset performance," in *Proc. IEEE Int. Symp. Antennas Propag.*, July 2010, pp. 1–4.

[17] J. Nielsen, B. Yanakiev, I. Bonev, M. Christensen, and G. Pedersen, "User influence on MIMO channel capacity for handsets in data mode operation," *IEEE Trans. Antennas Propag.*, vol. 60, no. 2, pp. 633–643, Feb. 2012.

[18] R. Vaughan and J. B. Andersen, *Channels, Propagation and Antennas for Mobile Communications*. The IEE, 2003.

[19] Z. N. Chen, *Antennas for Portable Devices*. John Wiley & Sons, Ltd, 2007.

[20] T. Brown, "Antenna diversity for mobile terminals," 2002, PhD thesis, University of Surrey, 2002. [Online]. Available: http://personal.ee.surrey.ac.uk/Personal/T.Brown/thesis.html

[21] C. Waldschmidt, C. Kuhnert, M. Pauli, and W. Wiesbeck, "Integration of MIMO antenna arrays into hand-helds," in *5th IEE Int. Conf. 3G Mobile Commun. Technol.*, 2004, pp. 16–23.

[22] P. Vainikainen, J. Holopainen, C. Icheln, O. Kivekäs, M. Kyrö, M. Mustonen, S. Ranvier, R. Valkonen, and J. Villanen, "More than 20 antenna elements in future mobile phones, threat or opportunity?" in *Proc. 3rd European Conf. Antennas Propag.*, Mar. 2009, pp. 2940–2943.

[23] C. A. Balanis, *Modern Antenna Handbook*. John Wiley & Sons, Inc., 2008.

[24] C. Rowell and E. Lam, "Mobile-phone antenna design," *IEEE Antennas Propag. Mag.*, vol. 54, no. 4, pp. 14–34, Aug. 2012.

[25] J. Villanen, J. Ollikainen, O. Kivekäs, and P. Vainikainen, "Coupling element based mobile terminal antenna structures," *IEEE Trans. Antennas Propag.*, vol. 54, no. 7, pp. 2142–2153, July 2006.

[26] J. Villanen, "Miniaturization and evaluation methods of mobile terminal antenna structures," Doctoral thesis, Helsinki University of Technology, 2007. [Online]. Available: http://lib.tkk.fi/Diss/2007/isbn9789512289646/

[27] R. Valkonen, "Impedance matching and tuning of non-resonant mobile terminal antennas," Doctoral thesis, Aalto University, 2013. [Online]. Available: https://aaltodoc.aalto.fi/handle/123456789/8898

[28] P. Vainikainen, J. Ollikainen, O. Kivekas, and K. Kelander, "Resonator-based analysis of the combination of mobile handset antenna and chassis," *IEEE Trans. Antennas Propag.*, vol. 50, no. 10, pp. 1433–1444, Oct. 2002.

[29] M. Cabedo-Fabres, E. Antonio-Daviu, M. Ferrando-Bataller, and A. Valero-Nogueira, "On the use of characteristic modes to describe patch antenna performance," in *Proc. IEEE Int. Symp. Antennas Propag.*, vol. 2, June 2003, pp. 712–715.

[30] J. Rahola and J. Ollikainen, "Optimal antenna placement for mobile terminals using characteristic mode analysis," in *Proc. 6th European Conf. Antennas Propag.*, Nov. 2006, pp. 1–6.

[31] M. Cabedo-Fabres, E. Antonino-Daviu, A. Valero-Nogueira, and M. Bataller, "The theory of characteristic modes revisited: A contribution to the design of antennas for modern applications," *IEEE Antennas Propag. Mag.*, vol. 49, no. 5, pp. 52–68, Oct. 2007.

[32] K. Fujimoto, *Mobile Antenna System Handbook*. Artech House, 2008.

[33] B. K. Lau, *MIMO: From Theory to Implementation (Alain Sibille, and Claude Oestges, and Alberto Zanella)*. Elsevier, 2011, Ch 10: Multiple Antenna Terminals.

[34] A. Paulraj, D. Gore, R. Nabar, and H. Bolcskei, "An overview of MIMO communications - a key to gigabit wireless," *Proc. IEEE*, vol. 92, no. 2, pp. 198–218, Feb. 2004.

[35] L. Zheng and D. Tse, "Diversity and multiplexing: a fundamental tradeoff in multiple-antenna channels," *IEEE Trans. Inf. Theory*, vol. 49, no. 5, pp. 1073–1096, May 2003.

[36] P.-S. Kildal and K. Rosengren, "Correlation and capacity of MIMO systems and mutual coupling, radiation efficiency, and diversity gain of their antennas: simulations and measurements in a reverberation chamber," *IEEE Commun. Mag.*, vol. 42, no. 12, pp. 104–112, Dec. 2004.

[37] K. Rosengren and P.-S. Kildal, "Radiation efficiency, correlation, diversity gain and capacity of a six-monopole antenna array for a MIMO system: theory, simulation and measurement in reverberation chamber," *IEE Proc. Microw., Antennas Propag.*, vol. 152, no. 1, pp. 7–16, Feb. 2005.

[38] D. M. Pozar, *Mirowave Engineering*, 3rd ed. John Wiley & Sons, Ltd, 2005.

[39] H. Wheeler, "Fundamental limitations of small antennas," *Proc. IRE*, vol. 35, no. 12, pp. 1479–1484, Dec. 1947.

[40] *IEEE Standard Definitions of Terms for Antennas*, IEEE Std 145-1993 Std.

[41] P.-S. Kildal and C. Orlenius, *Antenna Engineering Handbook (J.L. Volakis)*, 4th ed. New York: McGraw-Hill, 2007, Ch 58: Multipath Techniques for Handset/Terminal Antennas.

[42] N. Jamaly and A. Derneryd, "Efficiency characterisation of multi-port antennas," *Elect. Lett.*, vol. 48, no. 4, pp. 196–198, 16 2012.

[43] N. Jamaly, “Multiport antenna systems for space-time wireless communications,” Doctoral thesis, Chalmers University of Technology, 2013.

[44] T. Taga, “Analysis for mean effective gain of mobile antennas in land mobile radio environments,” *IEEE Trans. Veh. Technol.*, vol. 39, no. 2, pp. 117–131, May 1990.

[45] K. Kalliola, K. Sulonen, H. Laitinen, O. Kivekäs, J. Krogerus, and P. Vainikainen, “Angular power distribution and mean effective gain of mobile antenna in different propagation environments,” *IEEE Trans. Veh. Technol.*, vol. 51, no. 5, pp. 823–838, Sep. 2002.

[46] D. Yuan, D. Zhengwei, G. Ke, and F. Zhenghe, “A four-element antenna system for mobile phones,” *IEEE Antennas Wireless Propag. Lett.*, vol. 6, pp. 655–658, 2007.

[47] M. Jensen and Y. Rahmat-Samii, “Performance analysis of antennas for hand-held transceivers using FDTD,” *IEEE Trans. Antennas Propag.*, vol. 42, no. 8, pp. 1106–1113, Aug 1994.

[48] T. Taga, “Analysis of correlation characteristics of antenna diversity in land mobile radio environments,” *Electron. Commun. Japan (Part I: Communications)*, vol. 74, no. 8, pp. 101–116, 1991.

[49] L. Song and J. Shen, *Evolved Cellular Network Planning and Optimization for UMTS and LTE*, C. Press, Ed. Taylor & Francis Group, 2011.

[50] P.-S. Kildal and K. Rosengren, “Electromagnetic analysis of effective and apparent diversity gain of two parallel dipoles,” *IEEE Antennas Wireless Propag. Lett.*, vol. 2, pp. 9–13, 2003.

[51] A. Goldsmith, *Wireless Communications*. Cambridge University Press, 2005, Ch 7: Diversity.

[52] W. C. Lee, *Mobile Communications Engineering*. McGraw-Hill Professional, 1998, vol. 2.

[53] W.-Y. Lee, “Mutual coupling effect on maximum-ratio diversity combiners and application to mobile radio,” *IEEE Trans. Commun. Technol.*, vol. 18, no. 6, pp. 779–791, Dec. 1970.

[54] D. Gesbert, M. Shafi, D. shan Shiu, P. Smith, and A. Naguib, “From theory to practice: an overview of MIMO space-time coded wireless systems,” *IEEE J. Sel. Areas Commun.*, vol. 21, no. 3, pp. 281–302, Apr. 2003.

[55] P. Suvikunnas, J. Villanen, K. Sulonen, C. Icheln, J. Ollikainen, and P. Vainikainen, “Evaluation of the performance of multiantenna terminals using a new approach,” *IEEE Trans. Instrum. Meas.*, vol. 55, no. 5, pp. 1804–1813, Oct. 2006.

[56] P. Suvikunnas, J. Salo, L. Vuokko, J. Kivinen, K. Sulonen, and P. Vainikainen, “Comparison of MIMO antenna configurations: methods and experimental results,” *IEEE Trans. Veh. Technol.*, vol. 57, no. 2, pp. 1021–1031, Mar. 2008.

[57] J. Villanen, P. Suvikunnas, C. Icheln, J. Ollikainen, and P. Vainikainen, "Performance analysis and design aspects of mobile-terminal multi-antenna configurations," *IEEE Trans. Veh. Technol.*, vol. 57, no. 3, pp. 1664–1674, May 2008.

[58] D. Shiu, G. Foschini, M. Gans, and J. Kahn, "Fading correlation and its effect on the capacity of multielement antenna systems," *IEEE Trans. Commun.*, vol. 48, no. 3, pp. 502–513, 2000.

[59] P. Kildal, C. Orlenius, and J. Carlsson, "OTA testing in multipath of antennas and wireless devices with MIMO and OFDM," *Proc. IEEE*, vol. 100, no. 7, pp. 2145 –2157, July 2012.

[60] K. Sulonen, "Evaluation of performance of mobile terminal antennas," Doctoral thesis, Helsinki University of Technology, 2004. [Online]. Available: http://lib.tkk.fi/Diss/2004/isbn9512271648/

[61] Y. Okano and K. Cho, "Dependency of MIMO channel capacity on XPR around mobile terminals for multi-band multi-antenna," in *Proc. 2nd European Conf. Antennas Propag.*, Nov. 2007, pp. 1–6.

[62] A. Yamamoto, T. Hayashi, K. Ogawa, K. Olesen, J. Nielsen, N. Zheng, and G. Pedersen, "Outdoor urban propagation experiment of a handset MIMO antenna with a human phantom located in a browsing stance," in *IEEE 66th Veh. Technol. Conf.*, Oct. 2007, pp. 849–853.

[63] V. Plicanic, H. Asplund, and B. K. Lau, "Performance of handheld MIMO terminals in noise- and interference-limited urban macrocellular scenarios," *IEEE Trans. Antennas Propag.*, vol. 60, no. 8, pp. 3901–3912, Aug. 2012.

[64] P. Suvikunnas, "Methods and criteria for performance analysis of multiantenna systems in mobile communications," Doctoral thesis, Helsinki University of Technology, 2006. [Online]. Available: http://lib.tkk.fi/Diss/2006/isbn9512282976/

[65] V.-M. Kolmonen, "Propagation channel measurement system development and channel characterization at 5.3 ghz," Doctoral thesis, Aalto University, 2010. [Online]. Available: http://lib.tkk.fi/Diss/2010/isbn9789526030531/

[66] G. F. Pedersen and J. B. Andersen, "Handset antennas for mobile communications: integration, diversity and performance," *Review of Radio Science*, vol. 5, pp. 119–137, 1999.

[67] C. Waldschmidt, C. Kuhnert, S. Schulteis, and W. Wiesbeck, "MIMO handheld performance in the presence of a person," in *Proc. URSI Int. Symp. Electromagn. Theory*, 2004, pp. 81–83.

[68] D. Kemp and Y. Huang, "Antenna diversity and user interaction at 1800 mhz," in *Proc. IEEE Int. Symp. Antennas Propag.*, vol. 3A, July 2005, pp. 479–482.

[69] T. Zervos, A. Alexandridis, K. Peppas, F. Lazarakis, K. Dangakis, C. Soras, and B. Lindmark, "The influence of MIMO terminal user's hand on channel capacity," in *Proc. 1st European Conf. Antennas Propag.*, Nov. 2006, pp. 1–5.

[70] A. Michalopoulou, T. Zervos, K. Peppas, A. Alexandridis, F. Lazarakis, K. Dangakis, and D. Kaklamani, "The impact of the position of MIMO terminal user's hand on channel capacity," in *Proc. IEEE 18th Int. Symp. Pers., Indoor Mobile Radio Commun.*, Sep. 2007, pp. 1–5.

[71] G. Pedersen, J. Andersen, P. Eggers, J. Nielsen, H. Ebert, T. Brown, A. Yamamoto, T. Hayashi, and K. Ogawa, "Small terminal MIMO channels with user interaction," in *Proc. 2nd European Conf. Antennas Propag.*, Nov. 2007, pp. 1–6.

[72] U. Navsariwala, M. Schamberger, and N. Buris, "Impact of a user on the performance of MIMO antenna systems in small wireless devices," in *Proc. IEEE Int. Symp. Antennas Propag.*, July 2008, pp. 1–4.

[73] J. Valenzuela-Valdes, M. Garcia-Fernandez, A. Martinez-Gonzalez, and D. Sanchez-Hernandez, "The influence of efficiency on receive diversity and MIMO capacity for rayleigh-fading channels," *IEEE Trans. Antennas Propag.*, vol. 56, no. 5, pp. 1444–1450, May 2008.

[74] V. Plicanic, B. K. Lau, A. Derneryd, and Z. Ying, "Channel capacity performance of multi-band dual antenna in proximity of a user," in *IEEE Int. Workshop Antenna Technol.*, Mar. 2009, pp. 1–4.

[75] M. Okoniewski and M. Stuchly, "A study of the handset antenna and human body interaction," *IEEE Trans. Microw. Theory Techniques*, vol. 44, no. 10, pp. 1855–1864, 1996.

[76] G. Pedersen, K. Olesen, and S. Larsen, "Antenna efficiency of handheld phones," in *IEE Seminar Electromag. Assessment and Antenna Design Relating To Health Implications of Mobile Phones*, 1999, pp. 6/1–6/5.

[77] G. Pedersen, M. Tartiere, and M. Knudsen, "Radiation efficiency of handheld phones," in *IEEE 51th Veh. Technol. Conf.*, vol. 2, Tokyo, 2000, pp. 1381–1385.

[78] K. Boyle, "The performance of GSM 900 antennas in the presence of people and phantoms," in *Int. Conf. Antennas Propag.*, vol. 1, 2003, pp. 35–38.

[79] K. R. Boyle, Y. Yuan, and L. P. Ligthart, "Analysis of mobile phone antenna impedance variations with user proximity," *IEEE Trans. Antennas Propag.*, vol. 55, no. 2, pp. 364–372, Feb. 2007.

[80] M. Pelosi, O. Franek, M. Knudsen, M. Christensen, and G. Pedersen, "A grip study for talk and data modes in mobile phones," *IEEE Trans. Antennas Propag.*, vol. 57, no. 4, pp. 856–865, Apr. 2009.

[81] C.-H. Li, E. Ofli, N. Chavannes, and N. Kuster, "Effects of hand phantom on mobile phone antenna performance," *IEEE Trans. Antennas Propag.*, vol. 57, no. 9, pp. 2763–2770, Sep. 2009.

[82] *CTIA Test Plan for Mobile Station Over the Air Performance, Revision 3.1*, CTIA Wireless Association Std., January 2011.

[83] J. Holopainen, "Compact uhf-band antennas for mobile terminals: Focus on modelling, implementation and user interaction," Doctoral thesis, Aalto University, 2011. [Online]. Available: http://lib.tkk.fi/Diss/2011/isbn9789526040868/

[84] J. Ilvonen, O. Kivekäs, J. Holopainen, R. Valkonen, K. Rasilainen, and P. Vainikainen, "Mobile terminal antenna performance with the user's hand: Effect of antenna dimensioning and location," *IEEE Antennas Wireless Propag. Lett.*, vol. 10, pp. 772–775, 2011.

[85] C.-H. Li, E. Ofli, N. Chavannes, and N. Kuster, "The influence of the user hand on mobile phone antenna performance in data mode," in *Proc. 3rd European Conf. Antennas Propag.*, Mar. 2009, pp. 449–452.

[86] R. Harrington and J. Mautz, "Theory of characteristic modes for conducting bodies," *IEEE Trans. Antennas Propag.*, vol. 19, no. 5, pp. 622–628, Sep. 1971.

[87] M. Mustonen, "Multi-element antennas for future mobile terminals," Licentiate thesis, Helsinki University of Technology, 2008.

[88] M. Karaboikis, C. Soras, G. Tsachtsiris, and V. Makios, "Compact dual-printed inverted-f antenna diversity systems for portable wireless devices," *IEEE Antennas Wireless Propag. Lett.*, vol. 3, no. 1, pp. 9–14, Dec. 2004.

[89] A. Molisch and M. Win, "MIMO systems with antenna selection," *IEEE Microw. Mag.*, vol. 5, no. 1, pp. 46–56, Mar. 2004.

[90] V. Papamichael and C. Soras, "Generalised selection combining diversity performance of multi-element antenna systems via a stochastic electromagnetic-circuit methodology," *IET Microw., Antennas Propag.*, vol. 4, no. 7, pp. 837–846, July 2010.

[91] M. Webb, D. Gibbins, and M. Beach, "Slot antenna performance and signal quality in a smartphone prototype," *IEEE Antennas Wireless Propag. Lett.*, vol. 9, pp. 1053–1056, 2010.

[92] Z. Ying, "Antennas in cellular phones for mobile communications," *Proc. IEEE*, vol. 100, no. 7, pp. 2286–2296, July 2012.

[93] F. Belloni, V. Ranki, A. Kainulainen, and A. Richter, "Angle-based indoor positioning system for open indoor environments," in *6th Workshop Positioning, Navigation Commun.*, Mar. 2009, pp. 261–265.

[94] G. Park, M. Kim, T. Yang, J. Byun, and A. Kim, "The compact quad-band mobile handset antenna for the LTE700 MIMO application," in *Proc. IEEE Int. Symp. Antennas Propag.*, June 2009, pp. 1–4.

[95] S. Chaudhury, W. Schroeder, and H. Chaloupka, "Multiple antenna concept based on characteristic modes of mobile phone chassis," in *Proc. 2nd European Conf. Antennas Propag.*, Nov. 2007, pp. 1–6.

[96] H. Li, Y. Tan, B. K. Lau, Z. Ying, and S. He, "Characteristic mode based tradeoff analysis of antenna-chassis interactions for multiple antenna terminals," *IEEE Trans. Antennas Propag.*, vol. 60, no. 2, pp. 490–502, Feb. 2012.

[97] H. Li, B. K. Lau, Z. Ying, and S. He, "Decoupling of multiple antennas in terminals with chassis excitation using polarization diversity, angle diversity and current control," *IEEE Trans. Antennas Propag.*, vol. 60, no. 12, pp. 5947–5957, Dec. 2012.

[98] R. Martens, E. Safin, and D. Manteuffel, "Inductive and capacitive excitation of the characteristic modes of small terminals," in *Loughborough Antennas Propag. Conf.*, Nov. 2011, pp. 1–4.

[99] ——, "Selective excitation of characteristic modes on small terminals," in *Proc. 5th European Conf. Antennas Propag.*, Apr. 2011, pp. 2492–2496.

[100] J. Ilvonen, "Isolated antenna structures of mobile terminals," Master thesis, Helsinki University of Technology, 2009. [Online]. Available: http://lib.tkk.fi/Dipl/2009/urn100019.pdf

[101] J. Ilvonen, J. Holopainen, O. Kivekas, R. Valkonen, C. Icheln, and P. Vainikainen, "Balanced antenna structures of mobile terminals," in *Proc. 4th European Conf. Antennas Propag.*, Apr. 2010, pp. 1–5.

[102] J. Ilvonen, "Environment insensitive mobile terminal antennas," Licentiate thesis, Aalto University, 2012. [Online]. Available: http://lib.tkk.fi/Lic/2012/urn100596.pdf

[103] B. K. Lau and Z. Ying, "Antenna design challenges and solutions for compact MIMO terminals," in *IEEE Int. Workshop Antenna Technol.*, 2011, pp. 70–73.

[104] C.-Y. Pan, T.-S. Horng, W.-S. Chen, and C.-H. Huang, "Dual wideband printed monopole antenna for WLAN/WiMAX applications," *IEEE Antennas Wireless Propag. Lett.*, vol. 6, pp. 149–151, 2007.

[105] R.-A. Bhatti, Y.-T. Im, and S.-O. Park, "Compact PIFA for mobile terminals supporting multiple cellular and non-cellular standards," *IEEE Trans. Antennas Propag.*, vol. 57, no. 9, pp. 2534–2540, 2009.

[106] J. Ma, Y.-Z. Yin, J.-L. Guo, and Y.-H. Huang, "Miniature printed octaband monopole antenna for mobile phones," *IEEE Antennas Wireless Propag. Lett.*, vol. 9, pp. 1033–1036, 2010.

[107] C.-R. Lin, T.-C. Hung, H.-H. Chiang, J.-H. Huang, J.-S. Chen, and Y.-C. Lin, "A novel open slot monopole antenna with a coupling element for WiMAX 3.5 GHz applications," in *International Conference on Applications of Electromagnetism and Student Innovation Competition Awards*, 2010, pp. 250–253.

[108] S. Dossche, J. Romeu, and S. Blanch, "Decoupling and decorrelation of two closely spaced monopoles for optimum MIMO capacity," in *Proc. 1st European Conf. Antennas Propag.*, Nov. 2006, pp. 1–4.

[109] S.-C. Chen, Y.-S. Wang, and S.-J. Chung, "A decoupling technique for increasing the port isolation between two strongly coupled antennas," *IEEE Trans. Antennas Propag.*, vol. 56, no. 12, pp. 3650–3658, Dec. 2008.

[110] C.-Y. Chiu, C.-H. Cheng, R. Murch, and C. Rowell, "Reduction of mutual coupling between closely-packed antenna elements," *IEEE Trans. Antennas Propag.*, vol. 55, no. 6, pp. 1732–1738, June 2007.

[111] F.-G. Zhu, J.-D. Xu, and Q. Xu, "Reduction of mutual coupling between closely-packed antenna elements using defected ground structure," *Elect. Lett.*, vol. 45, no. 12, pp. 601–602, June 2009.

[112] B. K. Lau and J. Andersen, "Simple and efficient decoupling of compact arrays with parasitic scatterers," *IEEE Trans. Antennas Propag.*, vol. 60, no. 2, pp. 464–472, Feb. 2012.

[113] I. Gupta and A. Ksienski, "Effect of mutual coupling on the performance of adaptive arrays," *IEEE Trans. Antennas Propag.*, vol. 31, no. 5, pp. 785–791, Sep. 1983.

[114] B. Friedlander and A. Weiss, "Direction finding in the presence of mutual coupling," *IEEE Trans. Antennas Propag.*, vol. 39, no. 3, pp. 273–284, Mar. 1991.

[115] K. Dandekar, H. Ling, and G. Xu, "Effect of mutual coupling on direction finding in smart antenna applications," *Elect. Lett.*, vol. 36, no. 22, pp. 1889–1891, Oct. 2000.

[116] T. T. Zhang, H. T. Hui, and Y. Lu, "Compensation for the mutual coupling effect in the ESPRIT direction finding algorithm by using a more effective method," *IEEE Trans. Antennas Propag.*, vol. 53, no. 4, pp. 1552–1555, Apr. 2005.

[117] M. Eric, A. Zejak, and M. Obradovic, "Ambiguity characterization of arbitrary antenna array: type I ambiguity," in *Proc. IEEE 5th Int. Symp. Spread Spectrum Tech. Applicat.*, vol. 2, Sep. 1998, pp. 399–403.

[118] R. Harrington, "Sidelobe reduction by nonuniform element spacing," *IRE Trans. Antennas Propag.*, vol. 9, no. 2, pp. 187–192, Mar. 1961.

[119] M. Ozdemir, E. Arvas, and H. Arslan, "Dynamics of spatial correlation and implications on MIMO systems," *IEEE Commun. Mag.*, vol. 42, no. 6, pp. S14–S19, June 2004.

[120] A. Diallo, C. Luxey, P. Le Thuc, R. Staraj, and G. Kossiavas, "Study and reduction of the mutual coupling between two mobile phone PIFAs operating in the DCS1800 and UMTS bands," *IEEE Trans. Antennas Propag.*, vol. 54, no. 11, pp. 3063–3074, Nov. 2006.

[121] J.-Y. Pang, S.-Q. Xiao, Z.-F. Ding, and B.-Z. Wang, "Two-element PIFA antenna system with inherent performance of low mutual coupling," *IEEE Antennas Wireless Propag. Lett.*, vol. 8, pp. 1223–1226, 2009.

[122] P. Mookiah and K. Dandekar, "Metamaterial-substrate antenna array for MIMO communication system," *IEEE Trans. Antennas Propag.*, vol. 57, no. 10, pp. 3283–3292, Oct. 2009.

Errata

Publication III

In Section 4.4, p. 151, Fig. 6, the y-axis should be ‘Mutual Coupling (dB)’ instead of ‘Isolation (dB)’.

This thesis studies characterization method of multiple antennas in compact mobile terminals. The time-varying propagation environment and user's hand grip emulating the true scenario of the users in real-life environments are taken into account. The thesis has scientific contribution on introducing novel multi-antenna structures with elements ranging from two to eight, and frequencies ranging from 900 MHz UHF to 3500 MHz LTE bands. Selection of suitable antenna type and their locations on the terminal chassis are shown to be important. Based on author's experience, the proposed designs are particularly suitable for realizing a multi-element antenna structure that is tolerant to the user. Detailed analysis has also been carried out on the antenna topology on a mobile terminal and consideration of user interaction to ascertain the best use of antennas for radio direction finding application in mobile terminals.

Aalto-DD 146/2013

ISBN 978-952-60-5338-7
ISBN 978-952-60-5339-4 (pdf)
ISSN-L 1799-4934
ISSN 1799-4934
ISSN 1799-4942 (pdf)

Aalto University
School of Electrical Engineering
Department of Radio Science and Engineering
www.aalto.fi

BUSINESS + ECONOMY

ART + DESIGN + ARCHITECTURE

SCIENCE + TECHNOLOGY

CROSSOVER

DOCTORAL DISSERTATIONS